Li X, Yang HY, Giachelli CM. 2006. Role of the sodium-dependent phosphate cotransporter, Pit-1, in vascular smooth muscle cell calcification. Circ Res 98:905–912.

Liu S, Tang W, Zhou J, Stubbs JR, Luo Q, Pi M, Quarles LD. 2006. Fibroblast growth factor 23 is a counter-regulatory phosphaturic hormone for vitamin D. J Am Soc Nephrol 17:1305–1315.

Liu S, Vierthaler L, Tang W, Zhou J, Quarles LD. 2008. FGFR3 and FGFR4 do not mediate renal effects of FGF23. J Am Soc Nephrol 19:2342–2350.

Mizobuchi M, Ogata H, Hatamura I, Koiwa F, Saji F, Shiizaki K, Negi S, Kinugasa E, Ooshima A, Koshikawa S, Akizawa T. 2006. Up-regulation of Cbfa1 and Pit-1 in calcified artery of uraemic rats with severe hyperphosphataemia and secondary hyperparathyroidism. Nephrol Dial Transplant 21:911–916.

Nishida Y, Taketani Y, Yamanaka-Okumura H, Imamura F, Taniguchi A, Sato T, Shuto E, Nashiki K, Arai H, Yamamoto H, Takeda E. 2006. Acute effect of oral phosphate loading on serum fibroblast growth factor 23 levels in healthy men. Kidney Int 70:2141–2147.

Nowik M, Picard N, Stange G, Capuano P, Tenenhouse HS, Biber J, Murer H, Wagner CA. 2008. Renal phosphaturia during metabolic acidosis revisited: Molecular mechanisms for decreased renal phosphate reabsorption. Pflugers Arch 457:539–549.

Pande S, Ritter CS, Rothstein M, Wiesen K, Vassiliadis J, Kumar R, Schiavi SC, Slatapolsky E, Brown AJ. 2006. FGF-23 and sFRP-4 in chronic kidney disease and post-renal transplantation. Nephron Physiol 104:23–32.

Perwad F, Azam N, Zhang MY, Yamashita T, Tenenhouse HS, Portale AA. 2005. Dietary and serum phosphorus regulate fibroblast growth factor 23 expression and 1,25-dihydroxyvitamin D metabolism in mice. Endocrinology 146:5358–5364.

Quarles LD. 2008. Endocrine functions of bone in mineral metabolism regulation. J Clin Invest 118:3820–3828.

Saito H, Kusano K, Kinosaki M, Ito H, Hirata M, Segawa H, Miyamoto K, Fukushima N. 2003. Human fibroblast growth factor-23 mutants suppress Na+-dependent phosphate co-transport activity and 1alpha,25-dihydroxyvitamin D3 production. J Biol Chem 278:2206–2211.

Segawa H, Kawakami E, Kaneko I, Kuwahata M, Ito M, Kusano K, Saito H, Fukushima N, Miyamoto K. 2003. Effect of hydrolysis-resistant FGF23-R179Q on dietary phosphate regulation of the renal type-II Na/Pi transporter. Pflugers Arch 446:585–592.

Shimada T, Mizutani S, Muto T, Yoneya T, Hino R, Takeda S, Takeuchi Y, Fujita T, Fukumoto S, Yamashita T. 2001. Cloning and characterization of FGF23 as a causative factor of tumor-induced osteomalacia. Proc Natl Acad Sci USA 98:6500–6505.

Shimada T, Hasegawa H, Yamazaki Y, Muto T, Hino R, Takeuchi Y, Fujita T, Nakahara K, Fukumoto S, Yamashita T. 2004a. FGF-23 is a potent regulator of vitamin D metabolism and phosphate homeostasis. J Bone Miner Res 19: 429–435.

Shimada T, Kakitani M, Yamazaki Y, Hasegawa H, Takeuchi Y, Fujita T, Fukumoto S, Tomizuka K, Yamashita T. 2004b. Targeted ablation of Fgf23 demonstrates an essential physiological role of FGF23 in phosphate and vitamin D metabolism. J Clin Invest 113:561–568.

Urakawa I, Yamazaki Y, Shimada T, Iijima K, Hasegawa H, Okawa K, Fujita T, Fukumoto S, Yamashita T. 2006. Klotho converts canonical FGF receptor into a specific receptor for FGF23. Nature 444:770–774.

Villa-Bellosta R, Ravera S, Sorribas V, Stange G, Levi M, Murer H, Biber J, Forster IC. 2009. The Na+–Pi cotransporter PiT-2 (SLC20A2) is expressed in the apical membrane of rat renal proximal tubules and regulated by dietary Pi. Am J Physiol Renal Physiol 296:F691–F699.

Virkki LV, Biber J, Murer H, Forster IC. 2007. Phosphate transporters: A tale of two solute carrier families. Am J Physiol Renal Physiol 293:F643–F654.

Weber TJ, Liu S, Indridason OS, Quarles LD. 2003. Serum FGF23 levels in normal and disordered phosphorus homeostasis. J Bone Miner Res 18:1227–1234.

Westerberg PA, Linde T, Wikstrom B, Ljunggren O, Stridsberg M, Larsson TE. 2007. Regulation of fibroblast growth factor-23 in chronic kidney disease. Nephrol Dial Transplant 22:3202–3207.

Biochimica et Biophysica Acta 1812 (2011) 326–332

Contents lists available at ScienceDirect

Biochimica et Biophysica Acta

journal homepage: www.elsevier.com/locate/bbadis

Molecular characterization of tissue-nonspecific alkaline phosphatase with an Ala to Thr substitution at position 116 associated with dominantly inherited hypophosphatasia

Yoko Ishida, Keiichi Komaru [1], Kimimitsu Oda *

Division of Oral Biochemistry, Niigata University Graduate School of Medical and Dental Sciences (Dentistry), 2-5274 Gakkocho-dori, Chuo-ku, Niigata 951-8514, Japan

ARTICLE INFO

Article history:
Received 5 October 2010
Received in revised form 30 November 2010
Accepted 2 December 2010
Available online 17 December 2010

Keywords:
Dominance
Genetic disease
Hypophosphatasia
Inborn error of metabolism
Tissue-nonspecific alkaline phosphatase

ABSTRACT

Mutations in the tissue-nonspecific alkaline phosphatase (TNSALP) gene are responsible for hypophosphatasia, an inborn error of bone and teeth metabolism associated with reduced levels of serum alkaline phosphatase activity. A missense mutation (c.346G>A) of TNSALP gene, which converts Ala to Thr at position 116 (according to standardized nomenclature), was reported in dominantly transmitted hypophosphatasia patients (A.S. Lia-Baldini et al. Hum Genet. 109 (2001) 99–108). To investigate molecular phenotype of TNSALP (A116T), we expressed it in the COS-1 cells or Tet-On CHO K1 cells. TNSALP (A116T) displayed not only negligible alkaline phosphatase activity, but also a weak dominant negative effect when co-expressed with the wild-type enzyme. In contrast to TNSALP (W, wild-type), which was present mostly as a non-covalently assembled homodimeric form, TNSALP (A116T) was found to exist as a monomer and heterogeneously associated aggregates covalently linked via disulfide bonds. Interestingly, both the monomer and aggregate forms of TNSALP (A116T) gained access to the cell surface and were anchored to the cell membrane via glycosylphosphatidylinositol (GPI). Co-expression of secretory forms of TNSALP (W) and TNSALP (A116T), which are engineered to replace the C-terminal GPI anchor with a tag sequence (*his*-tag or *flag*-tag), resulted in the release of heteromeric complexes consisting of TNSALP (W)-*his* and TNSALP (A116T)-*flag*. Taken together, these findings strongly suggest that TNSALP (A116T) fails to fold properly and forms disulfide-bonded aggregates, though it is indeed capable of interacting with the wild-type and reaching the cell surface, therefore explaining its dominant transmission.

1. Introduction

Hypophosphatasia is a genetic disease caused by various mutations in the tissue-nonspecific alkaline phosphatase (TNSALP) gene [1–4]. To date, a total of 224 mutations have been reported worldwide as of Oct. 2010 (http://www.sesep. uvsq.fr/03_hypo_ mutations.php). Hypophosphatasia is characterized by reduced levels of serum alkaline phosphatase activity and defective bone and teeth mineralization. One of two natural substrates which relate to clinical manifestation of hypophosphatasia, inorganic pyrophosphate is thought to play a crucial role as a negative regulator at the site of mineralization. That is, TNSALP enhances the mineralization by hydrolyzing pyrophosphate to phosphate, and therefore, decline in the activity due to mutations in the TNSALP gene leads to various degrees of hypomineralization [2,3]. Symptom of hypophosphatasia varies widely and in general its severity is inversely related to serum alkaline phosphatase levels of the patients. Clinically, hypophosphatasia is classified into five major categories depending on the age at diagnosis: perinatal, infantile, childhood, adult and odonto forms. Recently, the perinatal form is further divided into lethal and benign types [4]. Severe hypophosphatasia (perinatal and infantile forms) is transmitted in an autosomal recessive way, while mild hypophosphatasia (childhood, adult and odonto forms) is transmitted in a recessive or dominant way.

Severe hypophosphatasia patients are homozygote or compound heterozygotes with severe mutations, while mild form results from compound heterozygosity for severe and moderate mutations or single heterozygosity for severe mutations [5]. Mutations in TNSALP gene not only reduce the enzyme activity of TNSALP mutant proteins to a various degree, but also residual activities often exhibit different

Abbreviations: DMEM, Dulbecco's modified minimum essential medium; ER, endoplasmic reticulum; GPI, glycosylphosphatidylinositol; PI-PLC, phosphatidylinositol-specific phospholipase C; TNSALP, tissue-nonspecific alkaline phosphatase; TNSALP (A116T), TNSALP with an alanine to threonine substitution at position 116; TNSALP (D306V), TNSALP with an aspartate to valine substitution at position 306; TNSALP (W), the wild-type TNSALP

* Corresponding author. Tel.: +81 25 227 2827; fax: +81 25 227 2831.
E-mail address: oda@dent.niigata-u.ac.jp (K. Oda).
[1] Present address: Kitasato Junior College of Health and Hygienic Sciences, Minami-Uonuma 949-7241, Japan.

0925-4439/$ – see front matter © 2010 Elsevier B.V. All rights reserved.
doi:10.1016/j.bbadis.2010.12.002

enzymatic properties from TNSALP (W) [6], probably providing additional variability in clinical symptoms. Apart from their direct effects on the catalytic function, TNSALP mutant proteins display a different magnitude of trafficking defects. We, along with other groups, have reported that defective trafficking of TNSALP mutant protein contributes a molecular mechanism of hypophosphatasia [7–12]. In one extreme case where T is deleted at 1559 of TNSALP cDNA, this frame-shift TNSALP with an additional 80-amino acid extension at the C-terminus failed to be modified by glycosylphosphatidylinositol (GPI) and resultantly is released into the medium [13,14].

There is an increasing number of mild hypophosphatasia with a dominant negative effect [5,15–17]. These dominant-type TNSALP mutants suppress the enzyme activity of TNSALP (W) to a various degree when they are co-expressed in a cell [5,15–17]. Thus this inhibition of the enzyme activity implies that TNSALP mutant proteins with a dominant effect and TNSALP (W) are able to interact with each other and form heteromeric enzyme complexes. However, molecular characterization of dominantly inherited TNSALP mutations has not been studied in detail so far. In this report, we examined the molecular defect of TNSALP (A116T, according to standardized nomenclature, where the ATG initiator codon is numbered as 1). Extensive study on familial pedigree and its laboratory data unequivocally show that TNSALP (A116T) is dominantly transmitted [17,18]. Also, the co-expression data showed that TNSALP (A116T) inhibits TNSALP (W) albeit to a lesser degree compared to other dominant negative mutants such as TNSALP (D378V) and TNSALP (G63V) [17]. Surprisingly, our data indicate that the replacement of alanine with threonine at position116 of TNSALP (A116T) renders TNSALP incompetent to form a dimeric structure and resultant monomeric polypeptides associate with each other to become disulfide-bonded high-molecular mass aggregates. Moreover, we have also indicated that TNSALP (W) is trapped in the aggregate of TNSALP (A116T) when they are co-expressed.

2. Materials and methods

2.1. Materials

Express^{35}S^{35}S protein labeling mix (>1000 Ci/mmol) was obtained from Dupont-New England Nuclear (Boston, MA.), and^{14}C-methylated proteins and enhanced chemiluminescence (ECL®) Western blotting detection reagent, peroxidase-conjugated donkey anti-(rabbit IgG) and Protein A-Sepharose CL-4B from Amersham Pharmacia Biotech (Arlington Heights, IL, USA); pALTER®-MAX, Altered sites® II mammalian mutagenesis system from Promega (Madison, WI, U.S.A.); G418 and pansorbin from Calbiochem (La Jolla CA, U.S.A.); Lipofectamine Plus Reagent from Invitrogen (Carlsbad, CA, U.S.A.); phosphatidylinositol-specific phospholipase C (PI-PLC) from BIOMOL International, L.P. (Plymouth Meeting, PA, U.S.A.); aprotinin, baker's yeast alcohol dehydrogenase, bovine serum albumin, doxycycline, and ANTI-FLAG®M2 Agarose from Sigma Chemical Co. (St. Louis, MO.U.S.A.); Ni-NTA (nickel-nitrilotriacetic acid) resin and plasmid Midi-kit from Qiagen (Hilden, Germany); pTRE2 and BD® CHO-K1 Tet-On cell line and Tet system approved Fetal bovine serum from Clontech (Palo Alto, CA, U.S.A.); sulphosucciniimidyl N-(D-biotinyl)-6-aminohexane from Dojindo Laboratories (Kumamoto, Japan); antipain, chymostatin, elastatinal, leupeptin and pepstatin A from Protein Research Foundation (Osaka, Japan); bovine liver catalase and hygromycin from Wako Pure Chemicals (Tokyo, Japan). Antiserum against recombinant human TNSALP was raised in rabbits as described previously [19].

2.2. Plasmids and transfection

The pALTER-MAX® encoding TNSALP (W) was constructed as described previously [9]. Mutations were introduced at specific sites using Altered sites® II mammalian mutagenesis system essentially according to the manufacturer's protocol [10]. Oligonucleotides used are: TNSALP (A116T), 5′-CCCACACAGGTACGTAGTGGCGGTGCC-3′; TNSALP (W) *his*-tag, 5′-GCAGCAAGGCTGCCTGCCTAGTGATGGT-GATGGTGATGGCTGGCAGGAGCACA-3′; TNSALP (W or A116T) *flag*-tag, 5′-GCAGCAAGGCTGCCTGCCTACTTATCGTCGTCATCCTTGTAA-TCGCTGGCAGGAGCACA-3′. The DNA sequence of the mutation sites was verified by DNA sequence analysis. The cDNA encoding TNSALP (W) or TNSALP (A116T) was further subcloned into pTRE2 to establish stable cell lines. Transfection and screening of stable cell lines were performed essentially according to the manufacturer's protocol. Tet-On cells, which successfully produced TNSALP (W) or the mutant TNSALP in the presence of doxycycline, but not in its absence, were identified using immunofluorescence. Established Tet-On cells were cultured and passaged in the absence of doxycycline until they were used for experiments. For immunoblotting or immunofluorescence studies, the cells were cultured in the presence of 1 μg/ml doxycycline for 24 h before used. Alternatively, cells were cultured 0.2 μg/ml of doxycycline for 14 h before biosynthetic experiments. For transient expression, COS-1 cells [$(1.0–1.3)\times10^5$ cells/35-mm dish] were transfected with 0.8 μg of each plasmid using Lipofectamine Plus according to the manufacturer's protocol as described previously [10] and the transfected cells were incubated for 24 h in 5% CO_2/95% air incubator before use. COS-1 cells were cultured in Dulbecco's modified Eagle's minimum essential medium (DMEM) supplemented with 10% fetal bovine serum [10].

2.3. Metabolic labeling and immunoprecipitation

For pulse-chase experiments, cells were preincubated for 0.5–1 h in the methionine/cysteine-free DMEM and labeled with 50–100 μCi of [^{35}S] methionine/cysteine for 0.5 h in the fresh methionine/cysteine-free MEM. After a pulse period, cells were washed and chased in the DMEM as described previously [10]. After metabolic labeling, the medium was removed, and the cells were lysed in 0.5 ml of lysis buffer [1% (w/v) Triton X-100/0.5% (w/v) sodium deoxycholate/0.05% (w/v) SDS in PBS]. A protease inhibitors cocktail (antipain, aprotinin, chymostatin, elastatinal, leupeptin, pepstatin A) was added to cell lysates and media (10 μg each/ml). The lysates were incubated for 20 min at 37 °C to extract TNSALP. The lysates and media were subjected to immunoisolation as described previously [10]. The immune complexes/protein A beads were boiled in the absence or presence of 1% (v/v) 2-mercaptoethanol, and then analyzed by SDS/PAGE [9% (w/v) gels], followed by fluorography [7]. For sequential purification of soluble forms of heteromeric TNSALPs, the medium was adjusted to 20 mM imidazole and incubated with Ni-chelate resin in the presence of 20 mM imidazole. After washing the resin with PBS containing 20 mM imidazole, TNSALP-*his* was released with PBS containing 200 mM imidazole. This fraction was diluted 3-fold with PBS and mixed with anti-*flag* antibody beads. After washing with PBS containing 500 mM NaCl and then PBS, TNSALP-*flag* was released by boiling in the presence of SDS.

2.4. Miscellaneous procedures

Immunofluorescence for alkaline phosphatase was performed as described previously [9,10]. Electric transfer of proteins and subsequent procedures were described as before [19]. Proteins on membranes were detected with ECL® Western blotting detection reagents. Cell surface biotinylation and PI-PLC digestion were carried out as described previously [8,10]. Sucrose-density-gradient centrifugation was performed as described previously [8]. Protein and alkaline phosphatase assays were performed as described previously [7,10]. One unit of alkaline phosphatase activity is defined as nmoles of *p*-nitrophenylphosphate hydrolyzed per min at 37 °C.

3. Results

3.1. Transient expression of TNSALP (A116T) in COS-1 cells

In order to define the molecular property of TNSALP (A116T), the wild-type enzyme and this mutant protein were expressed in COS-1 cells ectopically. In contrast to TNSALP (W), TNSALP (A116T) exhibited only negligible alkaline phosphatase activity as shown in Fig. 1A. In agreement with the previous report [17], when co-expressed with the wild enzyme, the activity of TNSALP (W) was slightly suppressed by TNSALP (A116T), indicative of a dominant negative effect of the latter (Fig. 1B). We have previously shown that the wild-type enzyme is synthesized as a 66 kDa form with high mannose-type oligosaccharides and is converted to a 80 kDa mature form with complex-type oligosaccharides as it migrates from the endoplasmic reticulum (ER) to the Golgi apparatus and finally is localized on the cell surface as a GPI-anchored protein [7,20]. Besides, these two molecular species are thought to exist as a non-covalently assembled homodimer at least in transfected COS-1 cells [8].

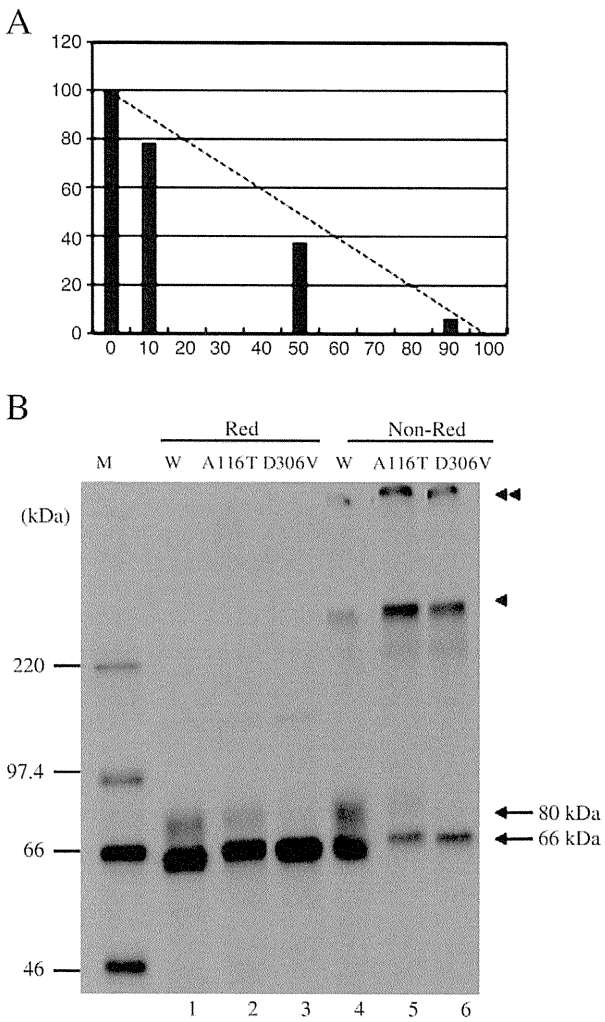

Fig. 1. Transient expression of TNSALP mutant proteins in COS-1 cells. (A) COS-1 cells were co-transfected with plasmids encoding TNSALP (W) or TNSALP (A116T) in various ratios (1: 0, 0.9: 0.1, 0.5: 0.5, 0.1: 0.9, 0: 1, *X* axis). The transfected cells were homogenized and assayed for alkaline phosphatase activity (expressed in % wild enzyme, *Y* axis). The dotted line expects variation of the enzyme activity in the recessive model. The values are the means of two independent experiments. (B) The cells expressing TNSALP (W) (lanes 1 and 4), TNSALP (A116T) (lanes 2 and 5) or TNSALP (D306V) (lanes 3 and 6) were steadily labeled with [^{35}S] methionine/cysteine for 3 h and lysed for immunoadsorption using anti-TNSALP antibody. Each immunoprecipitate was analyzed by SDS-PAGE under a reducing (lanes 1–3) or non-reducing condition (lanes 4–6), followed by fluorography. An arrowhead indicates the top of the resolving gel, while a double arrowhead indicates the top of the stacking gel. Left lane, ^{14}C-methylated protein markers of 200, 97.5, 66, 46 kDa, from the top of the gel.

Transfected cells were continuously labeled with [^{35}S] methionine/cysteine and then TNSALP was immunoprecipitated with an antibody against TNSALP, followed by SDS-PAGE under a reduced or non-reducing condition/fluorography. Both the 66 and 80 kDa forms were apparent in the cells expressing TNSALP (W) (Fig. 1, lane 1). Similarly, the 80 kDa mature form was also found in the cells expressing TNSALP (A116T) but not in the cells expressing TNSALP (D306V) (Fig. 1, lanes 2 and 3). The aspartic acid at position 306 is closely involved in the coordination of Ca^{2+} [21] and TNSALP (D306V) is retained in the endoplasmic reticulum (ER), followed by ubiquitination and degradation in proteasomes [10]. Under a non-reducing condition, a small amount of aggregates was detected even in the cell expressing TNSALP (W) (Fig. 1, lane 4), probably due to shortage of GPI precursors in transiently transfected cells [14]. On the other hand, larger amounts of the aggregate were found in the cells expressing TNSALP (A116T) or TNSALP (D306V) (Fig. 1, lanes 5 and 6).

3.2. Expression of TNSALP (A116T) in the Tet-On conditional expression system

To determine if the aggregation of TNSALP (A116T) is due to an excessive amount of this mutant generated in transiently transfected cells, we attempted to establish Tet-On CHO K1 cells expressing TNSALP (A116T) in response to doxycycline. Immunofluorescence pattern of Tet-On cells expressing TNSALP (A116T) was indistinguishable from that of the cells expressing TNSALP (W) (Fig. 2A). Both TNSALP (W) and the TNSALP mutant were observed on the cell surface only in the presence, but not in the absence of the antibiotic (data not shown). In accordance with the result of transiently transfected cells, TNSALP (A116T) lacked the enzyme activity as shown in Fig. 2B. Next, the steady state expression level of TNSALP (A116T) was assessed by immunoblotting. No protein band was observed in the absence of doxycycline. Only the 80 kDa band was detected in the cells expressing TNSALP (W) irrelevant to a reducing or non-reducing conditions (Fig. 3A, lanes 2 and 6). In contrast, in addition to the 80 kDa band a large amount of disulfide-bonded aggregate appeared in the established cell expressing the mutant protein (Fig. 3A, lanes 4 and 8). The presence of the 66 kDa form in the cells expressing TNSALP (A116T) but not TNSALP (W) raises a possibility that some part of TNSALP (A116T) exits from the ER only at a reduced rate (Fig. 3A, lanes 4 and 8). To further examine the aggregation state of TNSALP (W) and TNSALP (A116T), we subjected each cell lysate to sucrose-density-gradient centrifugation and then the fractions were analyzed by SDS-PAGE under a non-reducing condition as shown in Fig. 3B. Most of TNSALP (W) was recovered in fractions 7 and 8, where alcohol dehydrogenase (141 kDa) also appeared, demonstrating that TNSALP (W) exists as a homodimeric enzyme in Tet-On CHO. As SDS breaks this homodimeric structure even in the absence of a reducing reagent, the dimer was not detected on the gel. Markedly, a considerable fraction of TNSALP (A116T) appeared with bovine serum albumin (68 kDa) (Fig. 3B, fractions 5 and 6), strongly indicating that TNSALP (A116T) is incapable of assuming a correct tertiary structure and it tends to form disulfide-bonded aggregates with heterogeneous sizes, instead of a dimer.

3.3. Biosynthetic study of TNSALP (A116T) in the established cell line

To examine the biosynthesis of TNSALP (A116T) in detail, pulse-chase studies were carried out. The mutant protein is synthesized as the 66 kDa form (Fig. 4, lane 1), however, the disulfide-bonded aggregate started to appear during a 30-min pulse labeling time (Fig. 4, lanes 1 and 5) and was present throughout the chase periods (Fig. 4, lanes 6–8). This indicates that part of the newly synthesized

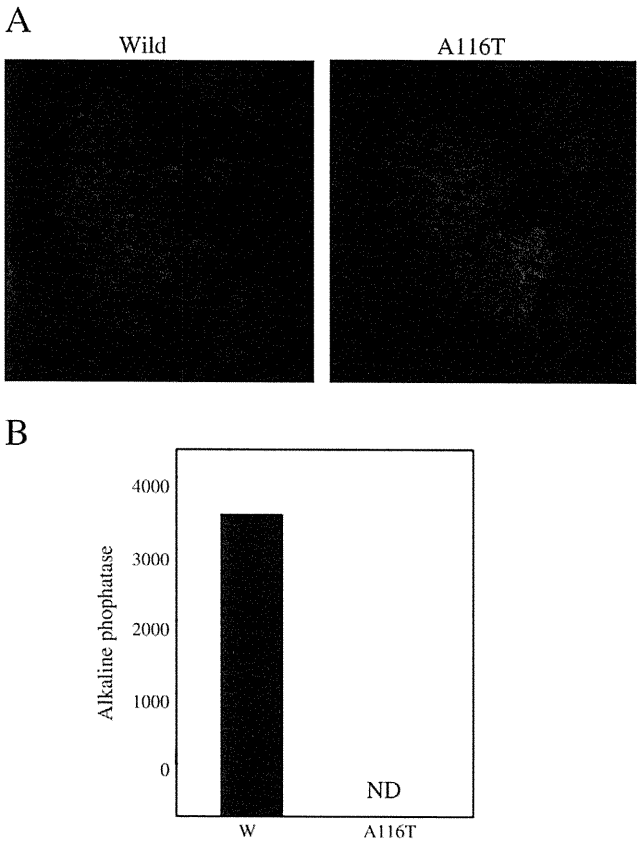

Fig. 2. Expression of TNSALP (W) and TNSALP (A116T) in established Tet-On cells. (A) Established cells harboring a pTRE2 encoding TNSALP (W) or TNSALP (A116T) were cultured for 24 h in the presence of doxycycline (1 μg/ml) and processed for immunofluorescence using anti-TNSALP serum. (B) Like in (A), the cells were induced to express TNSALP (W) or TNSALP (A116T). The cell homogenates were assayed for alkaline phosphatase activity. The values are the means of two independent experiments. The specific activity was expressed in unit mg^{-1} protein. ND denotes not detected.

66 kDa form of TNSALP (A116T) aggregates in the ER before it moves to the Golgi. At a 30-min chase period, the 80 kDa form was clearly detected under a reducing condition, while this mature form was less clear under a non-reducing condition (Fig. 3, lanes 2 and 6), indicating that a considerable amount of the 80 kDa form is in an aggregate state in the established cell. Also, we noticed that newly synthesized TNSALP (A116T) was decreased in its total intensity during the experiment. Longer chase experiments suggest that TNSALP (A116T) is less stable than the wild-type enzyme (Fig. 4B).

3.4. Cell surface appearance of disulfide-bonded aggregates of TNSALP (A116T)

The presence of the 80 kDa mature form in the aggregate raises a possibility that the high-molecular mass aggregate of TNSALP (A116T) synthesized in the ER moves to the Golgi, acquires terminal sugar residues during passage across the Golgi stack and finally is conveyed to the cell surface. Next, we examined the molecular species of TNSALP (A116T) exposed on the cell surface. Biosynthetic studies in combination with cell surface biotinylation (Fig. 5A) or digestion with PI-PLC (Fig. 5B) were performed. Not only the 80 kDa mature form, but also the aggregate on and near the top of the gel were reactive with a non-permeable biotinylation reagent. Furthermore, PI-PLC, which cleaves the GPI anchor portion from the TNSALP molecule, rendered the aggregate as well as the 80 kDa form released into the medium, indicating that both molecular species reside on the cell surface via the GPI anchor.

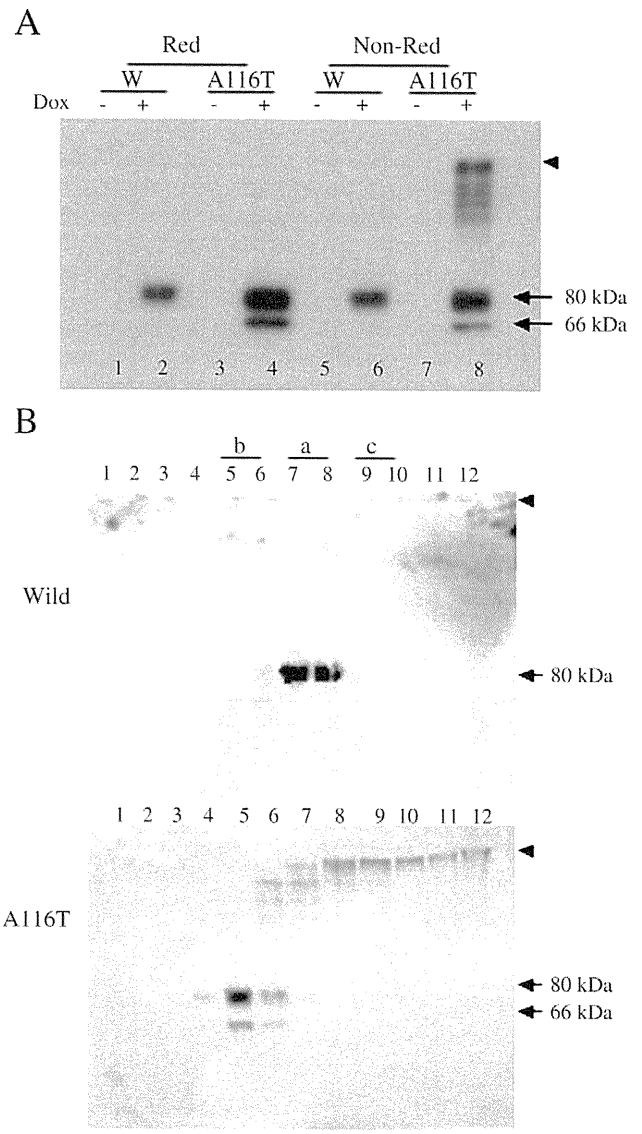

Fig. 3. Molecular size of TNSALP (W) and TNSALP (A116T). (A) The cells harboring pTRE2 encoding TNSALP (W) or TNSALP (A116T) were cultured for 24 h in the absence (lanes 1, 3, 5, and 7) or presence (lanes 2, 4, 6, and 8) of doxycycline (1 μg/ml) and then the cell homogenates (5 μg each) were analyzed by immunoblotting. An arrowhead indicates the top of the resolving gel. (B) The established cells were induced to express TNSALP (W) or TNSALP (A116T) like in (A). Each cell lysate was layered on the top of a linear sucrose gradient consisting of 5% (w/w) sucrose and 35% (w/w) sucrose and centrifuged at 4 °C for 18 h at 163,000g. Each 400 μl of fraction was collected from the top of the gradient (total 12 fractions). Each 20 μl of the fractions was subjected to SDS-PAGE under a non-reducing condition, followed by immunoblotting. Size marker: b (bovine serum albumin, 68 kDa, a (alcohol dehydrogenase, 141 kDa) and c (catalase, 250 kDa).

3.5. TNSALP (W) and TNSALP (A116T) interact with each other

Dominantly transmitted TNSALP mutant protein including TNSALP (A116T) are known to suppress the catalytic activity of TNSALP (W) to various degrees when they are expressed together (Fig. 1A) [15–17]. However, direct association between TNSALP (W) and a dominant negative TNSALP mutant protein has not been demonstrated to date. To confirm if TNSALP (W) and TNSALP (A116T) interact with each other, we co-expressed secretory versions of TNSALP (W) and TNSALP (A116T), which are modified by either a C-terminal *his* or *flag*tags (Fig. 6). TNSALP-*his* and TNSALP-*flag*, which possess each tag sequence instead of a C-terminal prosequence serving as a GPI anchor signal sequence, are secreted into the medium as a dimeric enzyme

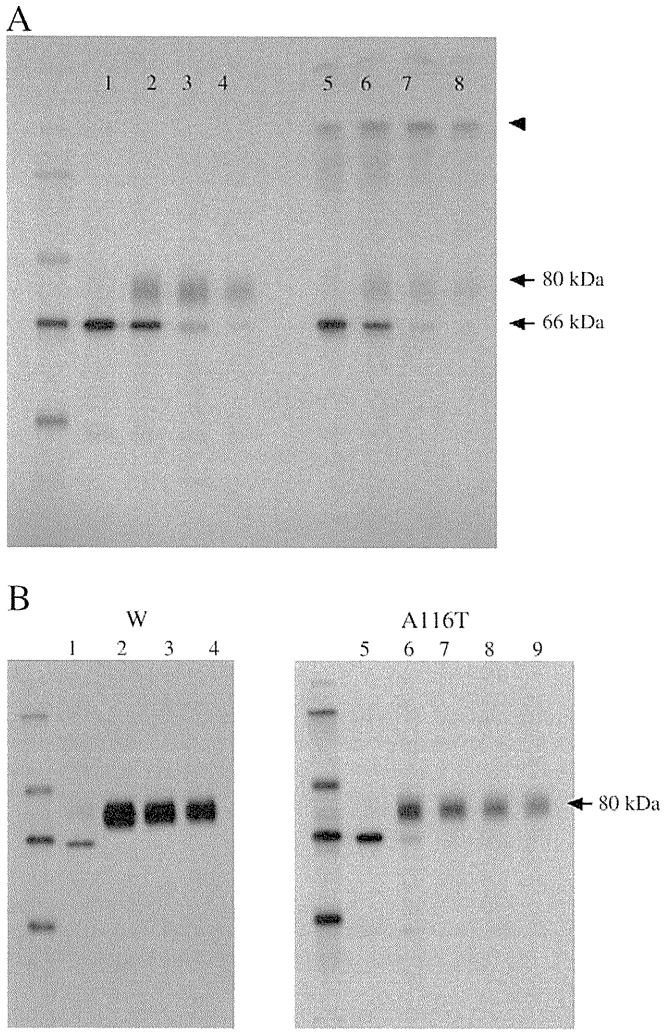

Fig. 4. Biosynthetic study of TNSALP (A116T). (A) The cells harboring pTRE2 encoding TNSALP (A116T) were cultured for 14 h in the presence of 0.2 μg/ml of doxycycline before experiments. The cells were pulse-labeled with [^{35}S] methionine/[^{35}S]cysteine for 30 min (lanes 1, 5), and chased for 30 min (lanes 2 and 6), 1 h (lanes 3 and 7) and 2 h (lanes 4 and 8) as described in Materials and methods. The immunoprecipitates were divided into two equal portions, followed by SDS-PAGE under reducing (lanes 1–4) or non-reducing condition (lanes 5–8)/fluorography. Left lane, the same ^{14}C-methylated protein markers as in Fig. 1. (B) The cells harboring pTRE2 encoding TNSALP (W) or TNSALP (A116T) were cultured like in A. The cells were pulse-labeled for 30 min (lane 1 and 5) and chased for 2 h (lane 6), 4 h (lanes 2 and 7), 6 h (lanes 3 and 8) and 8 h (lanes 4 and 8). The immunoprecipitates were analyzed by SDS-PAGE under a reducing condition/fluorography. Left lane, the same ^{14}C-methylated protein markers as in Fig. 1.

[6,19]. The levels of TNSALP in the media were more or less similar whether TNSALP (W)-*his* was co-expressed with TNSALP (W)-*flag* or TNSALP (A116T)-*flag* as assessed by direct immunoprecipitation using anti-TNSALP (Fig. 6, lanes 1 and 2). However, the aggregate was observed only in the culture medium of the cells expressing TNSALP (W)-*his* and TNSALP (A116T)-*flag* (Fig. 6, lane 2), implying that the GPI anchor portion of TNSALP (A116T) is not responsible for the formation of the aggregation. After being eluted with imidazole from the Ni-NTA agarose, the aggregate was no more evident (Fig. 5, lane 4). This is probably because TNSALP-*flag*/TNSALP-*flag* is not absorbed to the resin among the three possible combinations [TNSALP (W)-*his*/TNSALP (W)-*his*, TNSALP (W)-*his*/TNSALP (A116T)-*flag*, TNSALP (A116T) -*flag*/TNSALP-*flag*], resulting in the lower ratio of TNSALP (A116T)-*flag* to TNSALP (W)-*his* in the eluate. By a subsequent immunoadsorption using the anti-*flag* antibody, both the 80 kDa form and the aggregate were captured (Fig. 6, lane 6), indicating that TNSALP (W) is able to interact with the 80 kDa form non-covalently and the aggregate form of TNSALP (A116T) covalently, respectively.

4. Discussion

Based on 3D structure, TNSALP missense mutations associated with hypophosphatasia are classified as 1) active site or active site vicinity, 2) active site valley, 3) homodimer interface, 4) crown domain, 5) calcium site or calcium site vicinity and 6) others [21]. So far mutations with a dominant effect are restricted to three regions: active site, homodimer and the crown domain [5]. A116T is assigned to active site or active site vicinity, as serine at position 110 is an active center of TNSALP [21]. The patients heterozygous for TNSALP (A116T) displayed enamel hypoplasia and premature loss of fully rooted primary anterior teeth [18], corresponding to adult or odonto hypophosphatasia. Familial pedigree analysis demonstrated that TNSALP (A116T) is dominantly transmitted [17,18]. Milder phenotypes are probably attributed to its weak dominant negative effect on the wild-type enzyme, as shown by co-expression study (Fig. 1A) [17]. Initially we thought that TNSALP (W) and TNSALP (A116T) monomers form a simple non-covalently assembled hetero-dimer when they are co-expressed, however, their interaction turned out to be more complex.

To gain insight into the molecular mechanism of mild hypophosphatasia caused by this particular dominant negative mutation, we expressed TNSALP (A116T) as well as TNSALP (W) in COS-1 cells and Tet-On CHO K1 cells. Cell surface appearance of TNSALP (A116T) is indistinguishable from that of the wild enzyme as evaluated by immunofluorescence (Fig. 2). However, whether expressed in COS-1 cells transiently or Tet-On conditional expression system, TNSALP (A116T) does not exhibit measurable alkaline phosphatase activity. Besides, we found that TNSALP (A116T) tends to generate the disulfide-bonded high-molecular mass aggregate in contrast to a non-covalently assembled dimer structure of TNSALP (W) (Fig. 3A and B). The aggregate form of TNSALP (A116T) appeared in the cell within a 30-min pulse period, indicating that this aggregate is produced in the ER (Fig. 4). Surprisingly, the disulfide-bonded aggregate as well as the 66 kDa monomeric form of TNSALP (A116T) are transport-competent and appear on the cell surface as judged by cell surface biotinylation and PI-PLC digestion (Fig. 5).

To determine if TNSALP (A116T) is capable of interacting with TNSALP (W), we took an advantage that TNSALP (W) can be secreted as a homodimeric protein if its C-terminal prosequence serving as a GPI anchor signal is appropriately replaced with *his* or *flag*-tag [6,19]. Co-expression of TNSALP (W)-*his* and TNSALP (A116T)-*flag* in COS-1 cells allowed us to demonstrate that the wild and the mutant TNSALP interact with each other and are secreted into the medium (Fig. 6). Although the sequential affinity procedure is not quantitative, our finding strongly suggests that TNSALP (W) and TNSALP (A116T) form heterogeneous complexes and are anchored to the cell membrane via GPI in patients carrying this particular dominantly transmitted missense mutation.

Mornet's group has reported that dominant negative effects of TNSALP mutant proteins on the wild-type enzyme vary from one mutation to another [5,17]. TNSALP (D378V) and TNSALP (G63V) inhibit the enzyme activity far more strongly than TNSALP (A116T) does when co-expressed with TNSALP (W) [17]. On the other hand, TNSALP (G249V) exerts its dominant effect without suppressing the wild-type enzyme activity. TNSALP (G249V) likely sequesters the wild-type enzyme at the Golgi, thus blocking its cell surface appearance when co-expressed with the wild-type [22]. In this study our results demonstrated that the substitution of alanine with threonine at position 116 of TNSALP abrogates its tertiary structure. TNSALP (A116T) exits as a monomeric polypeptide and its randomly cross-linked aggregates via disulfide bonds. Considering that its dominant negative effect is weak [17], it is likely that only a small

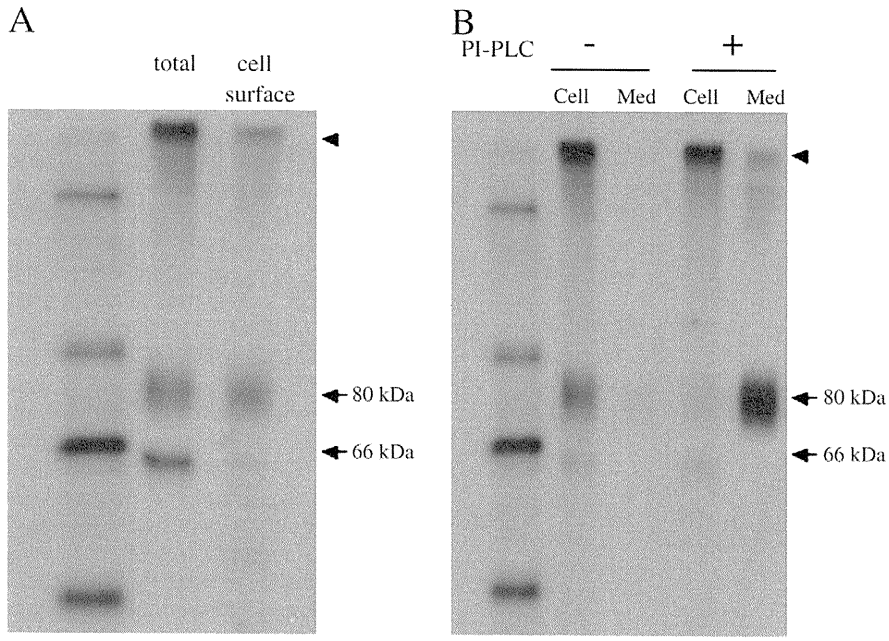

Fig. 5. Cell surface appearance of TNSALP (A116T). The cells harboring pTRE2 encoding TNSALP (A116T) were cultured for 14 h in the presence of 0.2 μg/ml of doxycycline and subjected to cell surface biotinylation or PI-PLC digestion. (A) After being steadily labeled with [^{35}S] methionine/cysteine for 3 h, the cells were washed and incubated with biotin succinimidylester on ice. The cell lysate was immunoprecipitated using anti-TNSALP antibody. The immune complexes were divided into two equal parts: One part is directly analyzed by SDS-PAGE under a non-reducing condition/fluorography as total TNSALP, while the other was boiled, diluted and further incubated with streptavidin beads before analysis (cell surface). Left lane, the same ^{14}C-methylated protein markers as in Fig. 1. An arrowhead indicates the top of the resolving gel. (B) The cells were steadily labeled like in (A) and further incubated in the absence (−) or presence (+) of PI-PLC in the DMEM. The cells and media were subjected to immunoprecipitation and then analyzed by SDS-PAGE under a non-reducing condition/fluorography. Left lane, the same ^{14}C-methylated protein markers as in Fig. 1. An arrowhead indicates the top of the resolving gel.

portion of newly synthesized TNSALP (W) may be associated with TNSALP (A116T) and entrapped in the aggregate when co-expressed, while the rest of the TNSALP (W) is able to assemble into the native homodimeric structure with a full enzyme activity. This result, along with others, leads to a speculation that molecular mechanisms whereby mild hypophosphatasia exerts its dominant negative effects are highly variable.

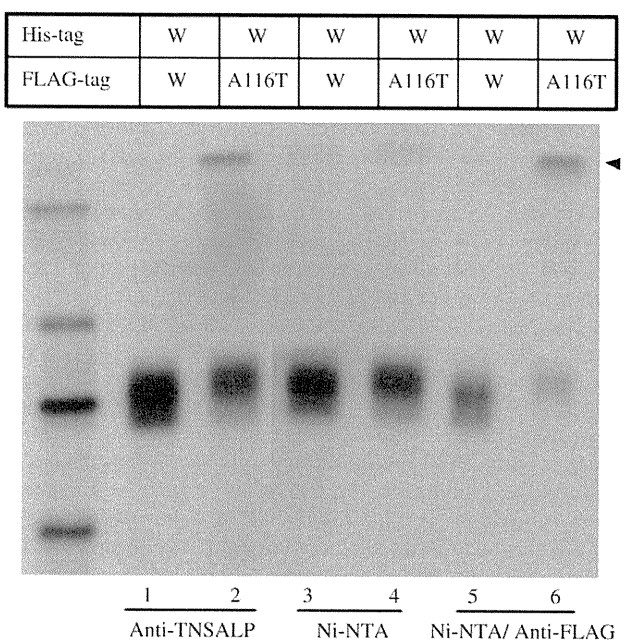

Fig. 6. Interaction between TNSALP (W) and TNSALP (A116T). COS-1 cells were transfected with cDNAs coding TNSALP (W)-*his* and TNSALP (W)-*flag* (lanes 1, 3 and 5) or TNSALP (W)-*his* and TNSALP (A116T)-*flag* (lanes 2, 4 and 6). The cells were labeled with [^{35}S] methionine/cysteine for 8 h. Each culture medium was collected and divided into three equal portions and was adsorbed with anti-TNSALP antibody (lanes 1 and 2), Ni-chelate beads (lanes 3 and 4) or Ni-chelate beads and subsequently with anti-*flag* antibody (lanes 5 and 6). Left lane, the same ^{14}C-methylated protein markers as in Fig. 1. An arrowhead indicates the top of the resolving gel.

Contrast to mild one with phenotypes of such as premature loss of deciduous teeth and pseudo-fracture, severe hypophosphatasia develops rickets or osteomalacia and sometimes hypercalcemia and vitamin B_6-dependent seizures [2–4]. The causative mutations for severe forms are transmitted in a recessive trait and also found to affect the TNSALP molecule to varying degrees, resulting in a complete loss or marked reduction of the catalytic function. Residual activities of these TNSALP mutants even exhibit different catalytic properties compared with the wild-type enzyme [6]. In addition, some TNSALP mutants showed folding and trafficking defects [7–12,20,23]. These broad effects of the mutations on the TNSALP molecule contribute the remarkably variable expressivity of this inborn error of metabolism. Obviously, more works will be necessary to be done until we will get a whole picture of molecular basis of hypophosphatasia.

There is no established medical treatment for hypophosphatasia. However, several attempts have recently been made to aim at developing the cure for this rare disease [24–26]. Especially, an enzyme replacement therapy using a soluble human recombinant TNSALP with a bone-targeted deca-aspartate motif is promising [24] and clinical trials are underway in Canada and the United States.

Acknowledgements

The authors thank Drs. N. Numa and M. Nasu-Naganuma and Ms. M. Okamura for technical assistance. We also thank Dr. S. Maruyama for preparing a figure.

This work was supported in part by a Grant from the Ministry of Health, Labour and Welfare of Japan (to K.O.), a Grant-in-Aid for Scientific Research from the Ministry of Education, Culture, Sports and Technology of Japan (to K.O.) and a Grant for Promotion of Niigata University Research Project (to Y.I.).

References

[1] H. Harris, The human alkaline phosphatases: what we know and what we don't know, Clin. Chim. Acta 186 (1989) 133–150.
[2] M.P. Whyte, Physiological role of alkaline phosphatase explored in hypophosphatasia, Ann. N.Y. Acad. Sci. 1192 (2010) 190–200.
[3] J.L. Millán, Mammalian alkaline phosphatases: from biology to applications in medicine and biotechnology, WILEY-VCH Verlag GmbH &Co. KGaA, Weinheim, 2006.
[4] E. Mornet, Hypophosphatasia, Orphanet J. Rare Dis. 2 (2007) 40.
[5] D. Fauvert, I. Brun-Heath, A.-S. Lia-Baldini, L. Bellazi, A. Taillandier, J.-L. Serre, P. de Mazancourt, E. Mornet, Mild forms of hypophosphatasia mostly result from dominant negative effect of severe alleles or from compound heterozygosity for severe and moderate alleles, BMC Med. Genet. 10 (2009) 51.
[6] S. Di Mauro, T. Manes, L. Hessle, A. Kozlenkov, J.M. Pizauro, M.F. Hoylaerts, J.L. Millán, J. Bone Miner. Res. 17 (2002) 1383–1391.
[7] H. Shibata, M. Fukushi, A. Igarashi, Y. Misumi, Y. Ikehara, Y. Ohashi, K. Oda, Defective intracellular transport of tissue-nonspecific alkaline phosphatase with an Ala162–Thr mutation associated with lethal hypophosphatasia, J. Biochem. (Tokyo) 123 (1998) 968–977.
[8] M. Fukushi-Irie, M. Ito, Y. Amaya, N. Amizuka, H. Ozawa, S. Omura, Y. Ikehara, K. Oda, Possible interference between tissue-non-specific alkaline phosphatase with an Arg54→Cys substitution and a counterpart with an Asp277→Ala substitution found in a compound heterozygote associated with severe hypophosphatasia, Biochem. J. 348 (2000) 633–642.
[9] M. Ito, N. Amizuka, H. Ozawa, K. Oda, Retention at the cis-Golgi and delayed degradation of tissue-non-specific alkaline phosphatase with an Asn153 to Asp substitution, a cause of perinatal hypophosphatasia, Biochem. J. 361 (2002) 473–480.
[10] Y. Ishida, K. Komaru, M. Ito, Y. Amaya, S. Kohno, K. Oda, Tissue-nonspecific alkaline phosphatase with an Asp289–Val mutation fails to reach the cell surface and undergoes proteasome-mediated degradation, J. Biochem. (Tokyo) 134 (2003) 63–70.
[11] I. Brun-Heath, A.-S. Lia-Baldini, S. Maillard, A. Taillandier, B. Utsch, M.E. Nunes, J.-L. Serre, E. Mornet, Delayed transport of tissue-nonspecific alkaline phosphatase with missense mutations causing hypophosphatasia, Eur. J. Med. Genet. 50 (2007) 367–378.
[12] G. Cai, T. Michigami, T. Yamamoto, N. Yasui, K. Satomura, M. Yamagata, M. Shima, S. Nakajima, S. Mushiake, S. Okada, K. Ozono, Analysis of localization of mutated tissue-nonspecific alkaline phosphatase proteins associated with neonatal hypophosphatasia using green fluorescent protein chimeras, J. Clin. Endocrinol. Metab. 83 (1998) 3936–3942.
[13] M. Goseki-Sone, H. Orimo, T. Iimura, H. Miyazaki, K. Oda, H. Shibata, M. Yanagishita, H. Watanabe, T. Shimada, S. Oida, Expression of the mutant (1735T-DEL) tissue-nonspecific alkaline phosphatase gene from hypophosphatasia patients, J. Bone Miner. Res. 13 (1998) 1827–1834.
[14] K. Komaru, Y. Ishida, Y. Amaya, M. Goseki-Sone, H. Orimo, K. Oda, Novel aggregate formation of a frame-shift mutant protein of tissue- nonspecific alkaline phosphatase is ascribed to three cysteine residues in the C-terminal extension. Retarded secretion and proteasomal degradation, FEBS J. 272 (2005) 1704–1717.
[15] H. Takanami, M. Goseki-Sone, H. Watanabe, H. Orimo, R. Hamatani, M. Fukushi-Irie, I. Ishikawa, The mutant (F310L and V365I) tissue-nonspecific alkaline phosphatase gene from hypophosphatasia, J. Med. Dent. Sci. 51 (2004) 67–74.
[16] H.L. Müller, M. Yamazaki, T. Michigami, T. Kageyama, E. Schünau, P. Schneider, K. Ozono, Asp^{361}Val mutant of alkaline phosphatase found in patients with dominantly inherited hypophosphatasia inhibits the activity of the wild-type enzyme, J. Clin. Endocrinol. Metab. 85 (2000) 743–747.
[17] A.S. Lia-Baldini, F. Muller, A. Taillandier, J.F. Gibrat, M. Mouchard, B. Robin, B. Simon-Bouy, J.L. Serre, A.S. Aylsworth, E. Bieth, S. Delanote, P. Freisinger, J.-C.C. Hu, H.-P. Krohn, M.E. Nunes, E. Mornet, A molecular approach to dominace in hypophosphatasia, Hum. Gent. 109 (2001) 99–108.
[18] J.-C.C. Hu, R. Plaetke, E. Mornet, C. Hang, X. Sun, H.F. Thomas, J.P. Simmer, Characterization of a family with dominant hypophosphatasia, Eur. J. Oral. Sci. 108 (2000) 189–194.
[19] K. Oda, Y. Amaya, M. Fukushi-Irie, Y. Kinameri, K. Ohsuye, I. Kubota, S. Fujimura, J. Kobayashi, A general method for rapid purification of soluble versions of glycosylphosphatidylinositol-anchored proteins expressed in insect cells: an application for human tissue-nonspecific alkaline phosphatase, J. Biochem. (Tokyo) 126 (1999) 694–699.
[20] N. Numa, Y. Ishida, M. Nasu, M. Sohda, Y. Misumi, T. Noda, K. Oda, Molecular basis of perinatal hypophosphatasia with tissue-nonspecific alkaline phosphatase bearing a conservative replacement of valine by alanine at position 406 Structural importance of the crown domain, FEBS J. 275 (2008) 2727–2737.
[21] E. Mornet, E. Stura, A.S. Lia-Baldini, T. Stigbrand, A. Ménez, M.H. Le Du, Structural evidence for a functional role of human tissue nonspecific alkaline phosphatase in bone mineralization, J. Biol. Chem. 276 (2001) 31171–31178.
[22] A.S. Lia-Baldini, I. Brun-Heath, C. Carrion, B. Simon-Bouy, J.-L. Serre, M.E. Numes, E. Mornet, A new mechanism of dominance in hypophosphatasia: the mutated protein can disturb the cell localization of the wild-type protein, Hum. Genet. 123 (2008) 429–432.
[23] M. Nasu, M. Ito, Y. Ishida, N. Numa, K. Komaru, S. Nomura, K. Oda, Aberrant interchain disulfide bridge of tissue-nonspecific alkaline phosphatase with an Arg433–Cys substitution associated with severe hypophosphatasia, FEBS J. 273 (2006) 5612–5624.
[24] J.L. Millán, S. Narisawa, I. Lemire, T.P. Loisel, G. Boileau, P. Leonard, S. Gramatikova, R. Terkeltaub, N.P. Camacho, M.D. McKee, P. Crine, M.P. Whyte, Enzyme replacement therapy for murine hypophosphatasia, J. Bone Miner. Res. 23 (2008) 777–787.
[25] Y. Katsube, N. Kotobuki, M. Tadokoro, R. Kanai, T. Taketani, S. Yamaguchi, H. Ohgushi, Restoration of cellular function of mesenchymal stem cells from a hypophosphatasia patient, Gene Ther. 17 (2010) 494–502.
[26] S. Yamamoto, H. Orimo, T. Matsumoto, O. Iijima, S. Narisawa, T. Maeda, J.L. Millán, T. Shimada, Prolonged survival and phenotypic correction of Akp2(−/−) hypophosphatasia mice by lentiviral gene therapy, J. Bone Miner. Res. 26 (2011) 135–142.

Circulating Levels of Soluble α-Klotho Are Markedly Elevated in Human Umbilical Cord Blood

Yasuhisa Ohata,* Hitomi Arahori,* Noriyuki Namba, Taichi Kitaoka, Haruhiko Hirai, Kazuko Wada, Masahiro Nakayama, Toshimi Michigami, Akihiro Imura, Yo-ichi Nabeshima, Yuji Yamazaki, and Keiichi Ozono

Department of Pediatrics (Y.O., H.A., N.N., T.K., H.H., K.W., K.O.), Osaka University Graduate School of Medicine, Suita 565-0871, Japan; Bone and Mineral Research (Y.O., T.M.) and Clinical Laboratory Medicine and Anatomic Pathology (M.N.), Osaka Medical Center and Research Institute for Maternal and Child Health, Izumi 594-1101, Japan; Department of Tumor Biology (A.I., Y.N.), Kyoto University Graduate School of Medicine, Kyoto 606-8501, Japan; Core Research for Evolutional Science and Technology (A.I., Y.N.), Science and Technology Corporation, Kawaguchi 332-0012, Japan; and Antibody Research Laboratories (Y.Y.), Kyowa Hakko Kirin Co., Ltd., Tokyo 194-8533, Japan

Context: Fetal serum levels of calcium and phosphate are higher than those in the maternal levels. Although α-Klotho is known to participate in calcium and phosphate metabolism in adults, its role in the perinatal period remains unknown.

Objective: This study aimed to determine the baseline levels of soluble α-Klotho in fetuses and compare them with those in neonates, mothers, and adults to clarify whether α-Klotho is involved in the fetal-specific regulation of calcium and phosphate metabolism.

Design and Setting: We conducted a cross-sectional evaluation of healthy babies (at birth and/or at 4 d after birth), their mothers, and adult volunteers at one hospital.

Participants: Twenty-one healthy mothers, their babies (23 in total, including two pairs of twins), and 25 adult volunteers participated in the study.

Main Outcome Measures: We measured the serum levels of soluble α-Klotho and fibroblast growth factor 23 (FGF23).

Results: In cord blood, the level of α-Klotho was markedly higher (3243 ± 1899 pg/ml) than levels in neonates at d 4 (582 ± 90 pg/ml), mothers (768 ± 261 pg/ml), and adult volunteers (681 ± 140 pg/ml) ($P < 0.001$), whereas the fetal level of FGF23 was lower than levels in the other subjects. The levels of soluble α-Klotho were negatively correlated with those of FGF23 in cord blood. Immunohistochemistry demonstrated that α-Klotho was predominantly expressed in syncytiotrophoblasts in normal term placenta.

Conclusion: Levels of soluble α-Klotho are markedly elevated in cord blood and might be useful as a biomarker for mineral metabolism in the fetus. (***J Clin Endocrinol Metab* 96: E943–E947, 2011**)

Fetal mineral homeostasis is regulated differently from adult homeostasis. The levels of serum calcium and phosphate in the fetus are higher than the maternal levels during late gestation. PTH and PTHrP are known to be involved in calcium homeostasis (1, 2). On the other hand, the regulatory mechanism of the fetal phosphate level is poorly understood (3).

The *α-Klotho* gene encodes a single-pass transmembrane protein, which was originally identified as an aging-related gene (4). In adults, α-Klotho contributes to the

ISSN Print 0021-972X ISSN Online 1945-7197
Printed in U.S.A.

doi: 10.1210/jc.2010-2357 Received October 6, 2010. Accepted March 2, 2011.
First Published Online March 16, 2011

* Y.O. and H.A. contributed equally to this work.

Abbreviations: FGF23, Fibroblast growth factor 23; 25-OHD, 25-hydroxyvitamin D; TRPV, transient receptor potential vanilloid.

regulation of calcium and phosphate homeostasis. In the parathyroid, α-Klotho binds to Na^+/K^+-ATPase to regulate PTH secretion and is involved in transepithelial calcium transport (5). α-Klotho is also involved in the activation of transient receptor potential vanilloid (TRPV) 5 in the kidney (6), indicating its central role in the maintenance of calcium homeostasis. In addition, α-Klotho participates in phosphate homeostasis by cooperating with fibroblast growth factor 23 (FGF23) and the FGF receptor (7). FGF23 reduces the serum phosphate level both by suppressing phosphate reabsorption and activating vitamin D in the proximal tubules (8–10).

Although *α-Klotho* is predominantly expressed in the kidney, parathyroid, and choroid plexus, it is also expressed in other tissues including the placenta (4). Its expression in the placenta has led us to hypothesize that α-Klotho might play a role in fetal mineral homeostasis as well as in postnatal homeostasis.

In addition to the transmembrane form, α-Klotho also exists in a soluble form. The soluble form, which is produced by the shedding of the transmembrane protein, is detectable in serum, cerebrospinal fluid, and urine (6, 11). Although soluble α-Klotho is considered to be a humoral factor (12), its regulatory mechanisms and functions are largely unknown, and it is considered that FGF23 signaling requires the transmembrane form of the protein.

Recently, a sandwich ELISA for soluble α-Klotho has been established (13). In the present study, we used this assay to measure the serum levels of soluble α-Klotho in cord blood at birth and compared them to the levels in neonates, mothers, and adults. We found that high levels of soluble α-Klotho are present in cord blood and analyzed the relationship between those of soluble α-Klotho and FGF23 in cord blood. To the best of our knowledge, this is the first report on the measurement of soluble α-Klotho levels in perinatal blood samples.

Subjects and Methods

Study participants

We recruited healthy pregnant women, their babies, and adult volunteers and obtained informed consent from all participants or their legal guardians. The institutional review board of Osaka University Hospital approved this study. The inclusion criteria were an unremarkable medical history, physical examination, and screening laboratory test results for endocrine and metabolic function. The exclusion criteria were premature or postmature infant delivery (gestational age under 37 wk and over 42 wk, respectively), and the neonate being light or heavy for their delivery date (birth weight under −1.5 SD and over 1.5 SD, respectively).

Twenty-one mothers and their babies (n = 23, including two pairs of twins) were enrolled. For comparison, 25 healthy adult volunteers ranging in age from 27 to 48 yr (11 males and 14 females) were also enrolled.

Blood analyses

After the delivery of the neonate, we immediately obtained cord blood samples from the umbilical vein, before the placenta was delivered. We also collected blood from the neonates at d 4 after birth in the morning and fasting morning blood from their mothers and the adult volunteers. The maternal blood was obtained within 24 h of the delivery. The participants were under no dietary restrictions during the study.

After we had collected the blood samples, we separated the serum instantly and stored it at −80 C until analysis. We measured the levels of serum soluble α-Klotho and intact FGF23 in all samples. The serum soluble α-Klotho levels were measured using an ELISA kit provided from Kyowa Hakko-Kirin (Tokyo, Japan) (13). The intra- and interassay coefficients of variation ranged from 2.7 to 9.8% (13). The serum levels of intact FGF23 were determined using a commercial sandwich ELISA kit (Kainos Laboratories, Inc., Tokyo, Japan) (14). Serum calcium, phosphate, intact PTH, 25-hydroxyvitamin D (25-OHD), albumin, and creatinine levels were also measured in the samples except for those from neonates. We corrected the levels of calcium in the samples displaying hypoalbuminemia (albumin < 4.0 g/dl) as reported previously (15).

Immunohistochemistry

Normal human placenta (gestational age, 38 wk) was obtained from an uncomplicated pregnancy. The specimen was fixed in 10% neutral buffered formalin, embedded in paraffin, and cut into 4-μm-thick sections. Antigen retrieval was performed using 10 mM citrate buffer (pH 5.9) for 15 min at 98 C. The sections were stained using anti-α-Klotho antibody (sc-22218; Santa Cruz Biotechnology, Santa Cruz, CA) and goat ImmunoCruz Staining System (Santa Cruz Biotechnology). The slides were counterstained with hematoxylin. Normal goat IgG was used as a negative control.

Statistical analyses

The results are expressed as the mean ± SD. We compared biochemical parameters and soluble α-Klotho and FGF23 levels among the groups by ANOVA, followed by the Tukey-Kramer method. The relationship between soluble α-Klotho and FGF23 in cord blood samples was analyzed using Pearson's correlation test.

All statistical analyses were conducted using JMP software version 8.0.1 (SAS Institute Inc., Cary, NC).

Results

Levels of soluble α-Klotho in cord blood are higher than those in neonates, mothers, and adults

The biochemical findings are shown in Table 1. Serum calcium, phosphate, intact PTH, 25-OHD, albumin, and creatinine levels were within the normal range in both the mother and adult groups (16). As previously reported, serum calcium and phosphate levels were significantly higher,

TABLE 1. Biochemical parameters

	Cord blood (n = 23)	Mother (n = 21)	Adult (n = 25)
Calcium (mg/dl)[a]	10.5 ± 0.43	9.44 ± 0.34[b]	9.42 ± 0.29[b]
Phosphate (mg/dl)	4.93 ± 0.65	3.66 ± 0.59[b]	3.62 ± 0.50[b]
Intact PTH (pg/ml)	7.11 ± 5.22	26.5 ± 12.2[b,f]	36.4 ± 9.80[b]
25-OHD (ng/ml)	8.95 ± 3.47	13.3 ± 6.45[d]	15.0 ± 4.43[c]
Albumin (g/dl)	3.53 ± 0.38	3.15 ± 0.42[c,e]	4.60 ± 0.27[b]
Creatinine (mg/dl)	0.49 ± 0.09	0.48 ± 0.08[e]	0.69 ± 0.10[b]

Data are expressed as mean ± SD and were compared among the cord blood group, mother group, and adult volunteer group using the ANOVA test.

[a] The calcium values were corrected using the following formula in cases involving hypoalbuminemia (Alb < 4.0 g/dl): corrected calcium (mg/dl) = measured calcium (mg/dl) + 4 − albumin (g/dl) (15).

[b] $P < 0.0001$ *vs.* cord blood; [c] $P < 0.01$ *vs.* cord blood; [d] $P < 0.05$ *vs.* cord blood; [e] $P < 0.0001$ *vs.* adult; [f] $P < 0.01$ *vs.* adult.

whereas serum intact PTH levels were lower in the cord blood than in the sera of the mother and adult volunteers (3).

The levels of soluble α-Klotho in the cord blood were markedly higher than those in the other groups ($P < 0.0001$) (Fig. 1A). The mean value for soluble α-Klotho in the cord blood was 3243 ± 1899 pg/ml, whereas those in the sera of the neonates at d 4, mothers, and adult volunteers were 582 ± 90, 768 ± 261, and 681 ± 140 pg/ml, respectively. There was no significant difference among the samples from neonates at d 4, mothers, and adults.

On the other hand, the levels of FGF23 in cord blood were significantly lower than those in other groups ($P < 0.0001$, *vs.* neonate and adult; $P < 0.0005$, *vs.* mother) (Fig. 1B). The mean value for FGF23 in cord blood was 8.61 ± 6.48 pg/ml, whereas those in the neonates, mothers, and adult volunteers were 28.4 ± 20.5, 26.7 ± 15.1, and 34.6 ± 7.69 pg/ml, respectively.

Negative correlation between the levels of soluble α-Klotho and FGF23 in cord blood samples

Then, using only the cord blood samples (n = 23), we examined the relationship between the levels of soluble α-Klotho and FGF23. We found that soluble α-Klotho levels were inversely correlated with FGF23 levels ($R^2 = 0.20$; $P < 0.05$) (Fig. 1C).

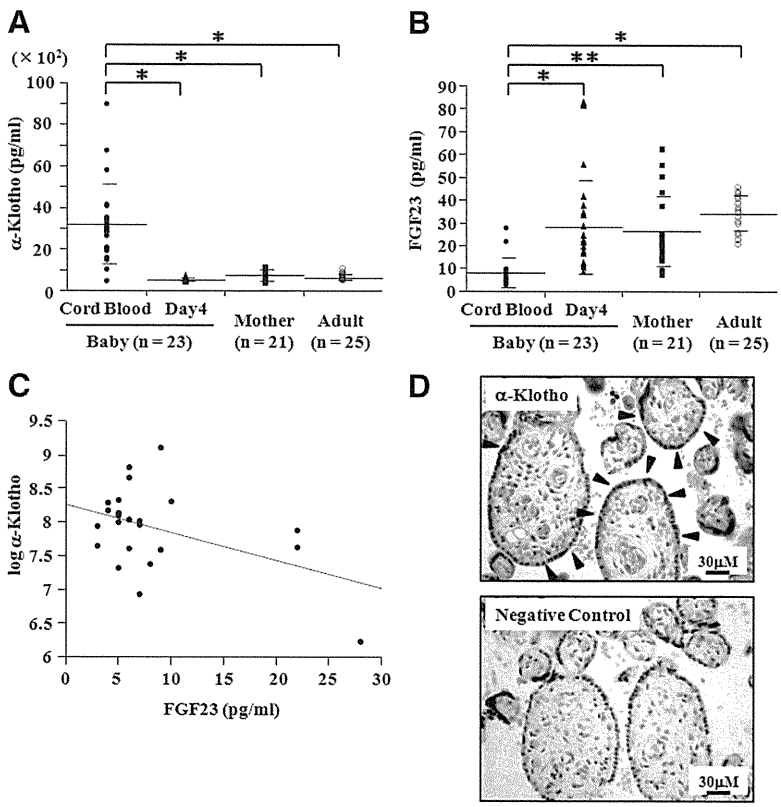

FIG. 1. A and B, Comparison of serum soluble α-Klotho (A) and FGF23 (B) levels among the cord blood, neonate at d 4, mother, and adult volunteer groups by ANOVA. *, $P < 0.0001$; **, $P < 0.0005$. *Closed circles*, *triangles*, *squares*, and *open circles* denote the values for the cord blood, neonate, mother, and adult volunteer groups, respectively. The *long and short bars* represent the mean and SD, respectively. C, Correlation of serum levels of α-Klotho with FGF23 in cord blood samples according to Pearson's correlation test. α-Klotho was log-transformed to reduce skewness. $R^2 = 0.20$; $P < 0.05$. D, Representative image of normal human term placenta stained with antibody against α-Klotho. α-Klotho was predominantly expressed in syncytiotrophoblasts (*arrowheads*). Normal goat IgG was used as a negative control.

Expression of α-Klotho in syncytiotrophoblasts in term placenta

Immunohistochemical staining demonstrated that α-Klotho was predominantly expressed in syncytiotrophoblasts with some expression in endothelium of fetal vessels and connective tissue of villi (Fig. 1D).

Discussion

In the current study, we found that the levels of soluble α-Klotho in cord vein blood that inflow to fetus after the exchange of gas and nutrients in the placenta were markedly higher than those in neonates, mothers, and adults (Fig. 1A). Immunohistochemical staining of the placenta revealed that syncytiotrophoblasts that originate from fetus predominantly expressed α-Klotho (Fig. 1D). Although we cannot exclude the possibility that other fetal tissues also contribute, it is likely that the syncytiotrophoblast is one of the major sources of the soluble α-Klotho circulating abundantly in the fetus. The lower level of soluble α-Klotho in neonates at d 4 compared with that in cord

blood supports the idea that the protein is derived from the placenta.

In contrast to the high levels of soluble α-Klotho, the levels of FGF23 in cord blood were lower than those in the other samples. This result was consistent with the findings of a previous report (17). Considering a report demonstrating that FGF23 expression in fetal rat bones was much lower than that in young adult rat bones (18), the low levels of FGF23 in cord blood might be due to the low expression of FGF23 in fetal tissues. In addition, it may suggest that the FGF23 in the mother's blood is not transferred to the fetus through the placenta.

We found a negative correlation between soluble α-Klotho and FGF23 levels in the cord blood samples. This result was also compatible with the data reported by Yamazaki *et al.* (13) in which samples from healthy children and adult volunteers were analyzed. Although the precise mechanism is unknown, the high level of soluble α-Klotho circulating in the fetus may contribute to the low level of intact FGF23 in cord blood.

We also performed multiple regression analysis and found that soluble α-Klotho was one of the determinants of the levels of phosphate (Supplemental Table 1, published on The Endocrine Society's Journals Online web site at http://jcem.endojournals.org). Serum calcium level also might be associated with that of α-Klotho, although the *P* value was 0.07. It has been reported that TRPV6 is involved in maternal-fetal calcium transport in mouse models (19). Moreover, Lu *et al.* have recently reported that α-Klotho activated not only TRPV5 but also TRPV6 (20). Given these results, soluble α-Klotho may contribute to the establishment of the fetomaternal calcium gradient also. However, considering the observation that the absence of α-Klotho in mice leads to hypercalcemia and hyperphosphatemia after birth (4), it remains to be determined whether the high levels of α-Klotho is an epiphenomenon in response to the higher serum calcium and phosphate, or is causing some of the biochemical features of fetuses. Even so, we can say that the measurement of soluble α-Klotho in cord blood as a biomarker might be useful in management of some genetic neonatal conditions such as hypercalcemia and hypophosphatemia. Measurement of calcium and phosphate during the perinatal period in the α-Klotho-deficient mice and generation of syncytiotrophoblast-specific α-Klotho-knockout mice might provide further insight into the roles of Klotho in fetal mineral metabolism.

In conclusion, the levels of soluble α-Klotho in cord blood were markedly high, and syncytiotrophoblasts in placenta were likely to be one of the major sources. Soluble α-Klotho in cord blood might be useful as a biomarker for calcium and phosphate metabolism in fetus.

Acknowledgments

We thank the staff of the neonate intensive care unit of Osaka University Hospital and all participants and their families.

Address all correspondence and requests for reprints to: Keiichi Ozono, M.D., Ph.D., 2-2 Yamadaoka, Suita, Osaka, 565-0871, Japan. E-mail: keioz@ped.med.osaka-u.ac.jp.

This work was supported by Grants-in-Aid for Scientific Research from the Japan Society for the Promotion of Science (to H.A.), Grants-in-Aid for Incurable Diseases from Osaka Medical Research Foundation for incurable diseases (to H.A.), and Grants-in-Aid for Intractable Disease from the Ministry of Health, Labor and Welfare of Japan (to T.M. and K.O.).

Disclosure Summary: Y.O., H.A., N.N., T.K., H.H., K.W., M.N., T.M., A.I., Y.N., and K.O. have nothing to declare. Y.Y. is an employee of Kyowa-Hakko Kirin Co., Ltd.

References

1. Simmonds CS, Karsenty G, Karaplis AC, Kovacs CS 2010 Parathyroid hormone regulates fetal-placental mineral homeostasis. J Bone Miner Res 25:594–605
2. Kovacs CS, Lanske B, Hunzelman JL, Guo J, Karaplis AC, Kronenberg HM 1996 Parathyroid hormone-related peptide (PTHrP) regulates fetal-placental calcium transport through a receptor distinct from the PTH/PTHrP receptor. Proc Natl Acad Sci USA 93:15233–15238
3. Kovacs CS 2008 Fetal calcium metabolism. In: Rosen CJ, ed. Primer on the metabolic bone diseases and disorders of mineral metabolism. 7th ed. Washington, DC: American Society for Bone and Mineral Research; 108–112
4. Kuro-o M, Matsumura Y, Aizawa H, Kawaguchi H, Suga T, Utsugi T, Ohyama Y, Kurabayashi M, Kaname T, Kume E, Iwasaki H, Iida A, Shiraki-Iida T, Nishikawa S, Nagai R, Nabeshima YI 1997 Mutation of the mouse klotho gene leads to a syndrome resembling ageing. Nature 390:45–51
5. Imura A, Tsuji Y, Murata M, Maeda R, Kubota K, Iwano A, Obuse C, Togashi K, Tominaga M, Kita N, Tomiyama K, Iijima J, Nabeshima Y, Fujioka M, Asato R, Tanaka S, Kojima K, Ito J, Nozaki K, Hashimoto N, Ito T, Nishio T, Uchiyama T, Fujimori T, Nabeshima Y 2007 α-Klotho as a regulator of calcium homeostasis. Science 316:1615–1618
6. Chang Q, Hoefs S, van der Kemp AW, Topala CN, Bindels RJ, Hoenderop JG 2005 The β-glucuronidase klotho hydrolyzes and activates the TRPV5 channel. Science 310:490–493
7. Urakawa I, Yamazaki Y, Shimada T, Iijima K, Hasegawa H, Okawa K, Fujita T, Fukumoto S, Yamashita T 2006 Klotho converts canonical FGF receptor into a specific receptor for FGF23. Nature 444:770–774
8. The ADHR Consortium 2000 Autosomal dominant hypophosphataemic rickets is associated with mutations in FGF23. Nat Genet 26:345–348
9. Shimada T, Mizutani S, Muto T, Yoneya T, Hino R, Takeda S, Takeuchi Y, Fujita T, Fukumoto S, Yamashita T 2001 Cloning and characterization of FGF23 as a causative factor of tumor-induced osteomalacia. Proc Natl Acad Sci USA 98:6500–6505
10. Segawa H, Kawakami E, Kaneko I, Kuwahata M, Ito M, Kusano K, Saito H, Fukushima N, Miyamoto K 2003 Effect of hydrolysis-resistant FGF23–R179Q on dietary phosphate regulation of the renal type-II Na/Pi transporter. Pflugers Arch 446:585–592
11. Imura A, Iwano A, Tohyama O, Tsuji Y, Nozaki K, Hashimoto N, Fujimori T, Nabeshima Y 2004 Secreted Klotho protein in sera and

CSF: implication for post-translational cleavage in release of Klotho protein from cell membrane. FEBS Lett 565:143–147
12. **Kurosu H, Yamamoto M, Clark JD, Pastor JV, Nandi A, Gurnani P, McGuinness OP, Chikuda H, Yamaguchi M, Kawaguchi H, Shimomura I, Takayama Y, Herz J, Kahn CR, Rosenblatt KP, Kuro-o M** 2005 Suppression of aging in mice by the hormone Klotho. Science 309:1829–1833
13. **Yamazaki Y, Imura A, Urakawa I, Shimada T, Murakami J, Aono Y, Hasegawa H, Yamashita T, Nakatani K, Saito Y, Okamoto N, Kurumatani N, Namba N, Kitaoka T, Ozono K, Sakai T, Hataya H, Ichikawa S, Imel EA, Econs MJ, Nabeshima Y** 2010 Establishment of sandwich ELISA for soluble α-Klotho measurement: age-dependent change of soluble α-Klotho levels in healthy subjects. Biochem Biophys Res Commun 398:513–518
14. **Yamazaki Y, Okazaki R, Shibata M, Hasegawa Y, Satoh K, Tajima T, Takeuchi Y, Fujita T, Nakahara K, Yamashita T, Fukumoto S** 2002 Increased circulatory level of biologically active full-length FGF-23 in patients with hypophosphatemic rickets/osteomalacia. J Clin Endocrinol Metab 87:4957–4960
15. **Fukumoto S, Namba N, Ozono K, Yamauchi M, Sugimoto T, Michigami T, Tanaka H, Inoue D, Minagawa M, Endo I, Matsumoto T** 2008 Causes and differential diagnosis of hypocalcemia—recommendation proposed by expert panel supported by ministry of health, labour and welfare, Japan. Endocr J 55:787–794
16. **Cunningham FG, Levono KJ, Bloom SL, Hauth JC, Rouse DJ, Spong CY** 2010 Williams obstetrics. 23rd ed. New York: McGraw-Hill
17. **Takaiwa M, Aya K, Miyai T, Hasegawa K, Yokoyama M, Kondo Y, Kodani N, Seino Y, Tanaka H, Morishima T** 2010 Fibroblast growth factor 23 concentrations in healthy term infants during the early postpartum period. Bone 47:256–262
18. **Yoshiko Y, Wang H, Minamizaki T, Ijuin C, Yamamoto R, Suemune S, Kozai K, Tanne K, Aubin JE, Maeda N** 2007 Mineralized tissue cells are a principal source of FGF23. Bone 40:1565–1573
19. **Suzuki Y, Kovacs CS, Takanaga H, Peng JB, Landowski CP, Hediger MA** 2008 Calcium channel TRPV6 is involved in murine maternal-fetal calcium transport. J Bone Miner Res 23:1249–1256
20. **Lu P, Boros S, Chang Q, Bindels RJ, Hoenderop JG** 2008 The β-glucuronidase klotho exclusively activates the epithelial Ca2+ channels TRPV5 and TRPV6. Nephrol Dial Transplant 23:3397–3402

Journal of Human Genetics (2011), 1–3

www.nature.com/jhg

COMMENTARY

Hypophosphatasia now draws more attention of both clinicians and researchers: A Commentary on prevelance of c. 1559delT in *ALPL*, a common mutation resulting in the perinatal (lethal) form of hypophosphatasias in Japanese and effects of the mutation on heterozygous carriers

Keiichi Ozono and Toshimi Michigami

Journal of Human Genetics advance online publication, 10 February 2011; doi:10.1038/jhg.2011.6

Hypophosphatsia is a skeletal disease due to an inborn error of metabolism characterized by deficient activity of the tissue-nonspecific alkaline phosphatase.[1,2] Alkaline phosphatase (ALP) is a membrane-bound metalloenzyme that consists of a group of isoenzymes encoded by four different gene loci: tissue-nonspecific, intestinal, placental and germ-cell ALP. Tissue-nonspecific alkaline phosphatase is expressed in almost all cells and three organs, liver, bone and kidney, have high activity of ALP. Thus, tissue-nonspecific alkaline phosphatase is also called ALP liver/bone/kidney (ALPL). The mouse counter part is called Akp2. Tissue-nonspecific alkaline phosphatase hydrolyzes inorganic pyrophosphate, an inhibitor of mineralization, and increases the local concentration of inorganic phosphate. Therefore, hypomineralization of skeleton and rachitic change of bone is associated with hypophosphatasia.

Hypophosphatasia is highly variable in its clinical expression. On the basis of the age of manifestation and its severity, hypophosphatasia is divided into six subtypes (Table 1). The most severe form of hypophosphatasia is a perinatal form, which is also called a lethal form. This form presents clinically either before or in the newborn period. The patients with this form exhibit severe defect of bone mineralization including craniotabes, bone deformity, short stature and narrow chest, and suffer from respiratory failure (Figure 1). However, some patients of this form can survive because of advances in neonatology.[3] Recently, non-lethal benign form of perinatal hypophosphatasia has been recognized, which is associated with no apparent defects of mineralization.[4,5] An infantile form is characterized by infantile onset and often associated with poor weight gain, hypercalcemia and respiratory difficulties. This form shows still rather high mortality. A childhood form is manifested at the age of 2 or 3 with premature loss of teeth, rachtic change of long bones and mild short stature. An adult form is sometimes associated with pathologic bone fracture and an odonto types means a form of only teeth manifestation. Diagnosis of hypophosphatasia is made on the basis of the clinical features, skeletal X-ray findings and low activity of ALP associated with elevation of its substrate, such as phosphoethanolamine, inorganic pyrophosphate and pyridoxal-5′-phosphate. We described diagnostic criteria of hypophosphatasia proposed by the Japanese Hypophosphatasia Study Group at http://www.bone.med.osaka-u.ac.jp/english/b5/.

Hypophosphatasia is usually inherited in an autosomal recessive manner, but can be expressed in an autosomal dominant manner in milder forms.[6] The *ALPL* gene is located on the short arm of chromosome 1 (1p36.1–p34), and contains 12 exons. The product consists of 507 amino acids including residues of the signal peptide. Hypophosphatasia is caused by various mutations in the *ALPL* gene. Currently, more than 200 mutations of the *ALPL* gene in patients with hypophosphatasia have been registered in the *ALPL* gene mutations database (http://www.sesep.uvsq.fr/Database.html). Most mutations described to date are missense mutations (80%), and the remainder was several deletion and insertion mutations of one to four nucleotides. Large deletions of the gene are rare (1.3%). Correlations of genotype and phenotype have been reported on the basis of clinical data of the patients with hypophosphatasia, enzymatic activity and computer-assisted modeling.[2]

We previously reported that the most and the second-most frequent mutations in Japanese patients are T1559del and F310L, respectively.[5] These mutations are renamed to c.1559delT and p.F327 L, respectively, based on the recent standardized nomenclature. Interestingly, both mutations are unique to Japanese. The common mutations, c.1559delT and p.F327 L, are associated with lethal and the perinatal non-lethal forms of hypophosphatasia, respectively. This is an example of

Professor K Ozono is at the Department of Pediatrics, Osaka University Graduate School of Medicine, 2-2 Yamadaoka, Suita, Osaka 565-0871, Japan and T Michigami is at the Department of Bone and Mineral Research Osaka Medical Center and Research Institute for Maternal and Child Health, 840 Murodo-cho, Izumi, Osaka 594-1101, Japan.
E-mail: keioz@ped.med.osaka-u.ac.jp

Table 1 Subtypes of hypophosphatasia and features

Subtypes	*Onset*	*Features*
Perinatal lethal	Fetus, neonate	Respiratory failure, severe mineralization defect, convulsion
Perinatal non-lethal	Fetus, neonate	Bone deformity
Infantile	Infant	Failure to thrive, hypercalcemia
Childhood	Child, especially toddlers	Premature loss of teeth, rickets-like changes
Adult	Adulthood	Fragile bone
Odonto	Not indicated	Teeth involvement only

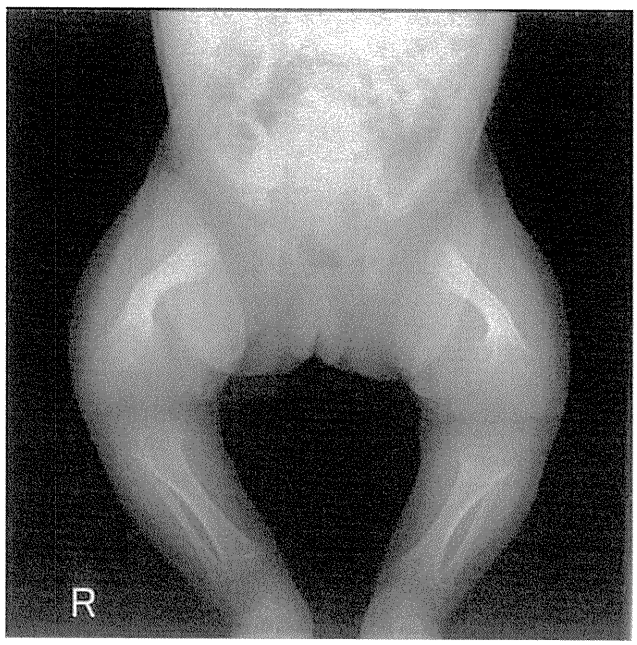

Figure 1 X-ray of legs of a neonate of hypophosphatasia. Severe rachitic changes of metaphysis of long bones are characteristic to hypophosphatasia. Bone deformity is also recognized.

the genotype–phenotype relationship, consistent with the enzymatic activity of the mutant ALP proteins; c.1559delT caused a complete loss of activity, whereas p.F327 L retains some residual activities. Therefore, genotyping patients with hypophosphatasia may help to predict their prognosis. In Europe, the E174K (renamed to p.E191K) mutation is reported to be frequent with a frequency of 31% in patients with mild hypophosphatasia.[7] As the E174K is associated with the same rare haplotype, the E174K mutation is surmised to be an ancestral mutation. However, the allele frequency of the E174K mutation is not investigated in normal population. In this issue of the journal, Watanabe *et al.*[8] reported prevelance of c. 1559delT in *ALPL*, a common mutation resulting in the perinatal (lethal) form of hypophosphatasias in Japanese. According to the article, the frequency is one per 480 (1/480), resulting in 1/920 000 homozygotes, because *de novo* mutation seems extremely rare. The frequency indicates more than one patient with this homozygous mutation is born per year in Japan, which has ~1 100 000 newborns per year. In our experience of examination of mutation in the *ALPL* gene in 42 patients with hypophosphatasia, homozygous mutation of c.1559delT was found in 17% patients. Thus, around seven patients with hypophosphatasia per year may be born in Japan based on the small number of examination. The carrier frequency for the mutant allele is estimated to be 1/25 in the Manitoba Mennonite community in Canada, which has the highest incidence rate for severe form of hypophosphatasia.[9]

There is no established medical treatment to cure hypophosphatasia, but there are some specific treatments for complications of hypophosphatasia.[1] In severe form of hypophosphasia, patients often suffer from intractable convulsions. This complication was also reported in $akp2^{-/-}$ mice.[10] The convulsion can be controlled by administration of vitamin B6 because abnormal metabolism of vitamin B6 leading to the deficient γ-aminobutyric acid in brain is observed in $akp2^{-/-}$ mice. In an infantile form of hypophosphatasia, patients tend to have hypercalcemia because of low bone formation. Low calcium-containing milk is recommended for hypercalcemia. Recently, treatment with parathyroid hormone 1–34, teriparatide, has been reported to improve bone formation, although its effect is still controversial.[11,12] Bone marrow transplantation has been reported to treat several patients with hypophosphatasia.[13] However, a method must be developed that improves the survival of donor mesenchymal cells in patients. Likewise, other congenital enzyme defect disorders, such as Hurler or Hunter disease, recombinant enzyme replacement therapy is being attempted in hypophosphatasia. Recombinant bone-targeted ALP therapy is effective in terms of mineralization and life-span in $akp2^{-/-}$ mice.[14] The therapy is now on clinical trial and expected to be available in near future.

1 Whyte, M. P. Physiological role of alkaline phosphatase explored in hypophosphatasia. Prolonged survival and phenotypic correction of Akp2(−/−) hypophosphatasia mice by lentiviral gene therapy. *Ann. N. Y. Acad. Sci.* **1192,** 190–200 (2010).
2 Mornet, E. Hypophosphatasia. *Orphanet. J. Rare. Dis.* **2,** 40 (2007).
3 Nakamura-Utsunomiya, A., Okada, S., Hara, K ., Miyagawa, S., Takeda, K., Fukuhara, R. *et al.* Clinical characteristics of perinatal lethal hypophosphatasia: a report of 6 cases. *Clin. Pediatr. Endocrinol.* **19,** 7–13 (2010).
4 Stevenson, D. A., Carey, J. C., Coburn, S. P., Ericson, K. L., Byrne, J. L., Mumm, S. *et al.* Autosomal recessive hypophosphatasia manifesting in utero with long bone deformity but showing spontaneous postnatal improvement. *J. Clin. Endocrinol. Metab.* **93,** 3443–3448 (2008).
5 Michigami, T., Uchihashi, T., Suzuki, A., Tachikawa, K., Nakajima, S. & Ozono, K. Common mutations F310L and T1559del in the tissue-nonspecific alkaline phosphatase gene are related to distinct phenotypes in Japanese patients with hypophosphatasia. *Eur. J. Pediatr.* **164,** 277–282 (2005).
6 Müller, H. L., Yamazaki, M., Michigami, T., Kageyama, T., Schönau, E., Schneider, P. *et al.* Asp361Val mutant of alkaline phosphatase found in patients with dominantly inherited hypophosphatasia inhibits the activity of the wild-type enzyme. *J. Clin. Endocrinol. Metab.* **85,** 743–747 (2000).
7 Hérasse, M., Spentchian, M., Taillandier, A. & Etienne, M. Evidence of a founder effect for the tissue-nonspecific alkaline phosphatase (TNSALP) gene E174K mutation in hypophosphatasia patients. *Eur. J. Hum. Genet.* **10,** 666–668 (2002).
8 Watanabe, A., Karasugi, T., Sawai, H., Naing, B. T., Ikegawa, S., Orimo, H. *et al.* Prevalence of c.1559delT in *ALPL*, a common mutation resulting in the perinatal (lethal) form of hypophosphatasia in Japanese and effects of the mutation on heterozygous carriers. *J. Hum. Genet.* (e-pub ahead of print 23 December 2010; doi:10.1038/jhg.2010.161).
9 Greenberg, C. R., Taylor, C. L., Haworth, J. C., Seargeant, L. E., Philipps, S., Triggs-Raine, B. *et al.* A homoallelic Gly317–>Asp mutation in ALPL causes the perinatal (lethal) form of hypophosphatasia in

Canadian mennonites. *Genomics.* **17**, 215–217 (1993).
10 Fedde, K. N., Blair, L., Silverstein, J., Coburn, S. P., Ryan, L. M., Weinstein, R. S. *et al.* Alkaline phosphatase knock-out mice recapitulate the metabolic and skeletal defects of infantile hypophosphatasia. *J. Bone. Miner. Res.* **14**, 2015–2026 (1999).
11 Whyte, M. P., Mumm, S. & Deal, C. Adult hypophosphatasia treated with teriparatide. *J. Clin. Endocrinol. Metab.* **92**, 1203–1208 (2007).
12 Gagnon, C., Sims, N. A., Mumm, S., McAuley, S. A., Jung, C., Poulton, I. J. *et al.* Lack of sustained response to teriparatide in a patient with adult hypophosphatasia. *J. Clin. Endocrinol. Metab.* **95**, 1007–1012 (2010).
13 Whyte, M. P., Kurtzberg, J., McAlister, W. H., Steele, A., Coburn, S. P., McAlister, W. H. *et al*: Marrow cell transplantation for infantile hypophosphatasia. *J. Bone. Miner. Res.* **18**, 624–636 (2003).
14 Millán, J. L., Narisawa, S., Lemire, I., Loisel, T. P., Boileau, G., Leonard, P. *et al.* Enzyme replacement therapy for murine hypophosphatasia. *J. Bone. Miner. Res.* **23**, 777–787 (2008).

JBC Papers in Press. Published on November 12, 2010 as Manuscript M110.148403
The latest version is at http://www.jbc.org/cgi/doi/10.1074/jbc.M110.148403

Cellular ATP synthesis mediated by type III sodium-dependent phosphate transporter *Pit-1* is critical to chondrogenesis

Atsushi Sugita[1, 5], Shinji Kawai[2], Tetsuyuki Hayashibara[3], Atsuo Amano[2], Takashi Ooshima[3], Toshimi Michigami[4], Hideki Yoshikawa[5], Toshiyuki Yoneda[1]

[1]Department of Biochemistry, [2]Department of Oral Frontier Biology, [3]Department of Pediatric Dentistry, Osaka University Graduate School of Dentistry, [4]Department of Bone and Mineral Research, Osaka Medical Center and Research Institute for Maternal and Child Health, Izumi, Osaka 594-1101, Japan, [5]Department of Orthopaedic Surgery, Osaka University Graduate School of Medicine, 1-8 Yamadaoka, Suita-Osaka 565-0871, Japan.

Running head: *Pit-1* regulation of late chondrogenesis

Address correspondence to: Toshiyuki Yoneda, D.D.S., Ph.D. 1-8 Yamadaoka, Suita-Osaka 565-0871, Japan. Fax: +81-6-6879-2890: E-mail: tyoneda@dent.osaka-u.ac.jp

Disturbed endochondral ossification in X-linked hypophosphatemia (XLH) indicates an involvement of phosphate (Pi) in chondrogenesis. We studied the role of the sodium-dependent Pi co-transporters (NPT), which are a widely-recognized regulator of cellular Pi homeostasis, and its downstream events in chondrogenesis using *Hyp* mice, the murine homologue of human XLH. *Hyp* mice showed reduced apoptosis and mineralization in hypertrophic cartilage. *Hyp* chondrocytes in culture displayed decreased apoptosis and mineralization compared with wild-type (WT) chondrocytes, while glycosaminoglycan synthesis, an early event in chondrogenesis, was not altered. Expression of the type III NPT *Pit-1* and Pi uptake were diminished and intracellular ATP levels were also reduced in parallel with decreased caspase-9 and caspase-3 activity in *Hyp* chondrocytes. The competitive NPT inhibitor phosphonoformic acid (PFA) and ATP synthesis inhibitor 3-bromopyruvate (3-BrPA) disturbed endochondral ossification with reduced apoptosis *in vivo* and suppressed apoptosis and mineralization in conjunction with reduced Pi uptake and ATP synthesis in WT chondrocytes. Overexpression of *Pit-1* in *Hyp* chondrocytes reversed Pi uptake and ATP synthesis and restored apoptosis and mineralization. Our results suggest that cellular ATP synthesis consequent to Pi uptake via *Pit-1* plays an important role in chondrocyte apoptosis and mineralization and that chondrogenesis is ATP-dependent.

Endochondral ossification is critical to the development and growth of mammalians. The process begins with condensation of undifferentiated mesenchymal cells and these cells differentiate into proliferating chondrocytes which express type II, type IX, type XI collagen and sulfated glycosaminoglycans (GAG) (1). Proliferating chondrocytes further differentiate into hypertrophic chondrocytes expressing type X collagen, undergo apoptosis, mineralize and ultimately replaced by bone. Disturbance of the endochondral ossification leads to a variety of skeletal disorders.

The genetic disease X-linked hypophosphatemia (XLH) is the most common form of inherited rickets in humans and is related to the dominant disorder of phosphate (Pi) homeostasis (2). XLH is shown to be caused by inactive mutations of the *PHEX* gene and characterized by hypophosphatemia secondary to renal Pi wasting, growth retardation due to disturbed endochondral ossification, osteomalacia resulting from reduced mineralization and abnormally-regulated vitamin D metabolism (3). *Hyp* mice also display similar biochemical and phenotypic abnormalities with human XLH including hypophosphatemia, osteomalacia and skeletal abnormalities. *Hyp* mice thus are a mouse homologue of the human XLH (4). Previous studies reported that *Hyp* mice exhibited disorganized hypertrophic cartilage with reduced apoptotic chondrocytes and hypomineralization (5). We have previously reported that osteoclast number was decreased in *Hyp* mice compared with wild-type (WT) mice and high-Pi diet partially restored this, showing that Pi influences osteoclastogenesis and suggesting this Pi effect on osteoclastogenesis may be associated with the pathogenesis of abnormal skeletogenesis in *Hyp* mice (6). However, it remains unclear whether disturbed Pi homeostasis influences endochondral ossification leading to abnormal skeletogenesis in *Hyp* mice. In this context, it is noted that intracellular Pi levels decrease and extracellular Pi

levels prominently increase from the proliferating to the hypertrophic zone during chondrogenesis (7-10), suggesting that cellular Pi levels are associated with chondrocyte differentiation.

Cellular Pi levels are controlled by the sodium-dependent Pi co-transporters (NPT) (11). Previous studies reported that the type III NPT (*Pit-1*) was expressed in hypertrophic chondrocytes during endochondral ossification in mice (12) and that the expression of the type IIa NPT (*Npt2a*) and *Pit-1* was also detected in chick chondrocytes (13). Moreover, it has been demonstrated that Pi modulates chondrocyte differentiation (14-19) and apoptosis (13,20).

Based on these earlier results, we hypothesized that the NPT/Pi system plays a critical role in the regulation of chondrocyte differentiation. We found that *Pit-1* expression in chondrocytes is decreased in *Hyp* mice compared to WT mice and that *Pit-1* regulates apoptosis and mineralization in chondrocytes through modulating intracellular ATP synthesis and apoptotic signaling activity. On the other hand, *Hyp* chondrocytes showed no changes in GAG synthesis, which is an early event in chondrogenesis. Our findings suggest that ATP synthesis mediated by Pi influx via *Pit-1* is critical in the regulation of late chondrogenesis including apoptosis and mineralization and that the differentiation of cartilage is an ATP-dependent event.

EXPERIMENTAL PROCEDURES

Animals - All mice used were of the C57BL/6J strain. Normal mice were purchased from Nihon-Dobutsu Inc. (Osaka, Japan). *Hyp* mice were initially obtained from The Jackson Laboratory (Bar Harbor, ME), and were produced by cross-mating homozygous *Hyp* females (*Hyp*/*Hyp*) to hemizygous *Hyp* males (*Hyp*/Y). All animal experiments were performed according to the guideline of the Institutional Animal Care and Use Committee of Osaka University Graduate School of Dentistry.

Isolation and culture of mouse growth plate chondrocytes - Growth plate chondrocytes were isolated from the ribs of 4-week-old normal and *Hyp* mice by sequential digestion with 0.2% trypsin (Invitrogen, Carlsbad, CA) for 30 minutes and 0.2% collagenase (Wako Pure Chemical Industries Ltd. Osaka, Japan) for 3 hours as previously report (21). Isolated cells were plated onto 100-mm tissue culture dishes at a density of $1x10^6$ cells in α-minimum essential medium (α-MEM: Sigma, St. Louis, MO) supplemented with 10% FCS (Valley Biomedical Inc., Winchester, VA), 2 mmol/L L-glutamine and 0.1 mg/mL kanamycin. Two days later, to induce chondrogenesis and cartilage nodule formation, cells were plated at $3x10^5$ cells/well onto 24-well plates or at $5x10^4$ cells/well on 96-well plates coated with type I collagen (Nitta Gelatin Inc, Osaka, Japan) and cultured in the differentiation medium consisting of Dulbecco's modified Eagle medium (DMEM: Sigma) supplemented with 10% FCS, 50 μg/mL ascorbic acid and 100 ng/mL recombinant human bone morphogenetic protein-2 (rhBMP-2, Astellas Pharma Inc. Tokyo, Japan) for 7 days. From day 5 to day 7, to promote matrix mineralization, 5 mM β-glycerophosphate was added to the differentiation medium.

Reverse transcription-polymerase chain reaction (RT-PCR) and real-time PCR - Total RNA from chondrocytes was prepared using RNeasy kit (QIAGEN Inc., Valencia, CA) and reverse-transcribed with SuperScript II reverse transcriptase (Invitrogen). The primer sequences for mouse Npt1, mouse Npt2a, GAPDH and β-actin are available on request. PCR assays were performed using Taq DNA Polymerase (New England Biolabs Inc., Ipswich, MA) and dNTP Mix (Promega Corp. Madison, WI). Real-time PCR assays were performed using a LightCycler system (Roche Diagnostics) according to the manufacturer's instructions. Each reaction was carried out with QIAGEN QuantiTect SYBR Green PCR Master Mix. The expression levels of mRNA are indicated as the relative expression normalized by GAPDH. The primer sequences are available on request. Each procedure was repeated at least four times to assess reproducibility.

Measurement of Na-dependent Pi uptake - Assay for Na-dependent Pi uptake by growth plate chondrocytes was performed essentially as described (22). Briefly, confluent cells cultured in 24 well Costar microtiter dishes were incubated in 2 ml of uptake solution (150 mmol/L NaCl, 1.0 mmol/L $CaCl_2$, 1.8 mmol/L $MgSO_4$, 10 mmol/L HEPES, pH 7.4) at 37°C for 5 min. Transport was then initiated by replacing the uptake solution with fresh uptake solution (2 ml), supplemented with 0.1 mmol/L KH_2PO_4, and containing 3 μCi/mL of $KH_2{}^{32}PO_4$ (MP Biomedicals Inc, Irvine, CA). Cells were then incubated for 5 min at 37°C, and the reaction was stopped by the addition of ice-cold uptake solution supplemented with 150 mmol/L choline chloride substitution for NaCl. The same solution was then used to wash the cells three times (2 ml per wash), dissolved in 0.2 N NaOH, and the ^{32}P activity was counted on a scintillation counter. As a control, Na-independent Pi transport was measured in the same way, except that NaCl was

replaced by choline chloride in the uptake solution. Data were expressed as nanomoles of Pi per milligram of cellular protein per 5 min and Na-dependent Pi transport was calculated by subtracting Na-independent Pi transport from total Pi transport.

Alcian blue staining - Cell layers in 24-well plates were fixed with 3.7% formaldehyde for 10 minutes and with 70% ethanol for 5 minutes at room temperature. After fixation, cells were incubated with 5% acetic acid (pH 1.0 adjusted with HCl) for 5 minutes and stained with 1% alcian blue dye (Wako Pure Chemical Industries Ltd.) in 5% acetic acid for 10 minutes. The alcian blue staining was quantified using an NIH Image 1.63 software.

Alizarin red staining - Cell layers in 24-well plates were fixed with 3.7% formaldehyde for 10 minutes and with 95% ethanol for 10 minutes at room temperature. After fixation, mineralized nodules were stained with 1% alizarin red-S (Wako Pure Chemical Industries Ltd.) at pH 6.4 for 10 minutes at room temperature. The stained samples were washed three times with water and then air dried. The alizarin red staining was quantified using an NIH Image 1.63 software.

Treatment with NPT inhibitor - In vitro: Chondrocytes were treated with phosphonoformic acid (PFA or foscarnet, Sigma), which is a competitive inhibitor of NPT (23), at concentrations of 10^{-5} M to 10^{-3} M in the differentiation medium from day 1 to day 7. *In vivo*: Mice received PFA as described (24). PFA injection (*ip*, 1,000 mg/kg body weight) was started at 21-day-old and daily injected for 10 days into C57BL/6J mice. Histological analysis was performed at 31-day-old. Control mice received vehicle PBS.

Knockdown of Npt2a and Pit-1 by siRNA - Chondrocytes were seeded at a density of $5x10^5$ cells in 100-mm tissue culture dishes in α-MEM supplemented with 10% FCS and 2 mmol/L L-glutamine. The sequences of Stealth RNAi duplex oligoribonucleotides for mouse *Npt*2a and mouse *Pit-1* are available on request. *Npt2a*-targeted, *Pit-1*-targeted, or negative control (medium GC, siNEGATIVE, Invitrogen) Stealth RNAi duplex oligoribonucleotides was added to 1 mL serum-free Opti-MEM I Reduced-Serum Medium (Invitrogen) in a final concentration of 24 nM respectively. In a separate tube 20 μL Lipofectamine RNAiMAX (Invitrogen) were diluted in 1 mL serum-free Opti-MEM I Reduced-Serum Medium. After adding the siRNA solution to the Lipofectamine solution, the final transfection mixture was incubated for 20 min at room temperature. This transfection mixture was applied to the cells. After 48 hours, RNA extraction was performed for RT-PCR and transfected chondrocytes were plated onto 24-well plates or 96-well plates to determine Pi-transport, intracellular ATP levels, caspase activity and apoptosis.

Pit-1 overexpression - The cDNA was subcloned into the 5'-XhoI-BamHI-3' site of pcDNA3.1/Zeo (Invitrogen). Cells were transfected using FuGENE™-6 (Roche Diagnostics Inc) according to the manufacturer's protocol. After 48 hours of transfection, RNA extraction was performed for RT-PCR or transfected chondrocytes were re-plated onto 24-well plates or 96-well plates to determine Pi-transport, intracellular ATP levels, caspase activity and apoptosis. The cDNA for mouse *Pit-1* in the plasmid pBluescript was a generous gift of Dr. Kenichi Miyamoto (University of Tokushima Graduate School, Tokushima, Japan).

Histology and TUNEL staining - Tibiae were harvested, washed with PBS, fixed with 4% paraformaldehyde in 0.1 M phosphate buffer (pH 7.4) overnight, decalcified in 4.13% EDTA at room temperature for 2 weeks, and embedded in paraffin. Four-micrometer-thick sections were made and stained with hematoxylin and eosin. Apoptotic cells were identified by using the DeadEnd Fluorometric TUNEL System (Promega Corp.). After treatment with 10 mg/mL proteinase K for 10 min at room temperature, sections were incubated with rTdT incubation buffer for 1 hour at 37°C, rinsed, counterstained with 1 μg/mL 4',6-Diamidino-2-phenylindole (DAPI, Vector Laboratories, Ltd., Burlingame, CA) and mounted with Fluoromount-G (Southern Biotechnology Associates Inc, Birmingham, AL). The green TUNEL emission was analyzed under fluorescein filter set to view the green fluorescence of fluorescein at 520 nm and blue DAPI at 460 nm.

Measurement of apoptotic cell death - DNA fragmentation was measured using Cell Death Detection ELISA PLUS kit (Roche Diagnostics Inc), which detects the cytoplasmic histone-associated DNA fragments (mono- and oligonucleosomes) by photometric enzyme-immunoassay. Briefly, after differentiation of chondrocytes in 96-well plates, cell lysates were used for ELISA procedure, following the manufacture's protocol. DNA fragmentation was quantified at 405 nm. Results were normalized to cellular protein concentration.

Measurement of caspase-9 and caspase-3 activity - Activity of caspase-3 and caspase-9 was measured using the Caspase-Glo 3/7 Assay kit (Promega) and the Caspase-Glo 9 Assay kit (Promega) according to the manufacturer's instructions. Chondrocytes were cultured at a density of 5 x 10^4 cells/well for 5 days in 96-well plates in the differentiation medium and processed for caspase-9 and caspase-3 activity assays. The luminescence was measured using a luminometer (TD-20/20, Tuner Designs, Sunnyvale, CA). Results were normalized to cellular protein concentration.

Measurement of intracellular ATP levels - Intracellular ATP levels were measured by using ATP Assay kit (Calbiochem, Darmstadt, Germany). This assay utilizes luciferase to catalyze the formation of light from ATP and luciferin. Luminescence was measured using a TD-20/20 luminometer. Chondrocytes were cultured at a density of 5 x 10^4 cells/well for 24 hours in 24-well plates and processed for ATP bioluminescence assays. Results were normalized to cellular protein concentration.

Treatment with ATP synthesis inhibitor - In vitro: 3-bromopyruvate (3-BrPA, Sigma), a strong alkylating agent that abolishes cell ATP production via the inhibition of both glycolysis and oxidative phosphorylation (25-27), was added at 10^{-6} M~10^{-5} M in the differentiation medium from day 1 to day 7. *In vivo*: 3-BrPA (20 μg/kg of body weight) was intraperitoneal injected daily for 10 days into C57BL/6J mice. Control mice received vehicle PBS.

Statistical Analysis - Data were presented as mean +/- SEM. Raw data were analyzed by Mann-Whitney's U test or one-way analysis of variance followed by a post hoc test (Fisher's projected least significant difference) (StatView, SAS Institute Inc., Cary, NC) with a significance level of $p < 0.05$.

RESULTS

Reduced apoptosis and mineralization in growth plate cartilage in Hyp mice - It has been reported that apoptosis is a prerequisite to mineralization of chondrocytes (28). Previous studies including ours have reported that the growth plate cartilage in *Hyp* mice is hypomineralized (5,6). We, therefore, examined apoptosis in the growth plate cartilage in *Hyp* mice compared to WT mice. Histological examination revealed that hypertrophic cartilage was elongated and disorganized in *Hyp* mice (Figure 1 A, left). In conjunction with this, TUNEL staining showed decreased apoptosis in hypertrophic cartilage in *Hyp* mice (Figure 1A, right and Figure 1B). Consistent with these *in vivo* results, chondrocytes isolated from *Hyp* mice (*Hyp* chondrocytes) in culture showed decreased apoptosis assessed by DNA fragmentation using a commercially-available ELISA kit (Figure 1C) and mineralization determined by alizarin red staining (Figure 1D, bottom). Quantification of alizarin red staining was shown in Figure 1F. However, GAG synthesis that takes place at an early stage of chondrogenesis was not altered in *Hyp* chondrocytes as determined by alcian blue staining (Figure 1D, top) Alcian blue staining was quantified in Figure 1E.

Cellular events involved in reduced apoptosis in Hyp chondrocytes - Since activation of caspase-9 and caspase-3 is an important step that leads to apoptosis, the activity of caspase-9 and caspase-3 was next determined in WT and *Hyp* chondrocytes in culture. The activity of caspase-9 (Figure 2A) and caspase-3 (Figure 2B) was significantly decreased in *Hyp* chondrocytes. Adenosine triphosphate (ATP) has been reported to be critical in the activation of caspase-9 and caspase-3 (29, 30). Accordingly, we determined intracellular ATP levels in WT and *Hyp* chondrocytes and found that intracellular ATP levels in *Hyp* chondrocytes were significantly reduced compared with WT chondrocytes (Figure 2C). Collectively, these results suggest that decreased ATP levels impaired caspase signals and following apoptosis in *Hyp* chondrocytes.

Disturbed Pi homeostasis in Hyp chondrocytes - It has been described that Pi (polyphosphate) is a source of ATP (31). Accordingly, we next examined whether Pi uptake was changed in *Hyp* chondrocytes. As expected, we found that Pi uptake was significantly less in *Hyp* chondrocytes than WT chondrocytes (Figure 3A). Since cellular Pi uptake is under the control of NPT (11), NPT expression in *Hyp* chondrocytes was subsequently determined. RT-PCR showed that the type III NPT *Pit-1* expression was decreased in *Hyp* chondrocytes (Figure 3B) and real-time PCR demonstrated *Pit-1* expression was reduced at early stages of chondrocyte culture (Figure 3C). Consistent with our results, previous studies also reported that an increase in *Pit-1* expression at early stage was associated with late chondrocyte differentiation (16, 18). On the other hand, there was no difference in the type II *Npt2a* expression between WT and *Hyp* chondrocyte (Figure 3B and Figure 3D). The type I *Npt1* expression was not